

AD A 039 146

12
nw

AD

EDGEWOOD ARSENAL CONTRACT REPORT

EC-CR-76094

**DETERMINATION OF SUBPICOGRAM AMOUNTS
OF CHEMICAL AGENTS IN THE ATMOSPHERE
PHASE II**

Final Comprehensive Report

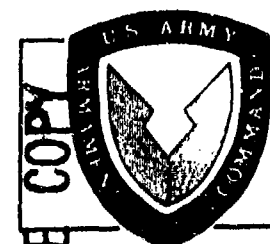
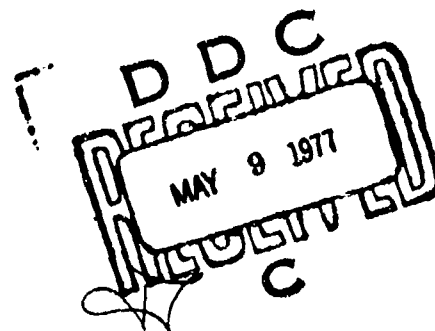
by

Gilbert A. St. John (Project Leader)
Michael Anbar (Project Supervisor)

February 1977

STANFORD RESEARCH INSTITUTE
Menlo Park, California 94025

Contract DAAA15-75-C-0132



DEPARTMENT OF THE ARMY
Headquarters, Edgewood Arsenal
Aberdeen Proving Ground, Maryland 21010



Approved for public release; distribution unlimited.

DDC FILE COPY

BEST

AVAILABLE

COPY

DISCLAIMER

The findings of this report are not to be construed as an official Department of the Army position unless so designated by other authorized documents.

DISPOSITION

Destroy this report when no longer needed. Do not return it to the originator.

18 19 REPORT DOCUMENTATION PAGE		READ INSTRUCTIONS BEFORE COMPLETING FORM	
1. REPORT NUMBER EC CR-76094	2. GOVT ACCESSION NO.	3. RECIPIENT'S CATALOG NUMBER	
4. TITLE (and Subtitle) 6 DETERMINATION OF SUBPICOGAM AMOUNTS OF CHEMICAL AGENTS IN THE ATMOSPHERE. PHASE II.		5. TYPE OF REPORT & PERIOD COVERED 9 Final Comprehensive rept. May 1975 - May 1976	
7. AUTHOR(s) 10 Gilbert A./St. John Michael/Anbar		6. PERFORMING ORG. REPORT NUMBER SRI Project PYU-4250	
9. PERFORMING ORGANIZATION NAME AND ADDRESS Stanford Research Institute Menlo Park, California 94025		8. CONTRACT OR GRANT NUMBER(s) 15 DAAA15-75-C-0132	
11. CONTROLLING OFFICE NAME AND ADDRESS Commander, Edgewood Arsenal Attn: SAREA-TS-R Aberdeen Proving Ground, Maryland 21010		10. PROGRAM ELEMENT, PROJECT, TASK AREA & WORK UNIT NUMBERS	
14. MONITORING AGENCY NAME & ADDRESS (if diff. from Controlling Office) Commander, Edgewood Arsenal Attn: SAREA-CL-DD Aberdeen Proving Ground, Maryland 21010 Charles S. Harden, Contract Project Officer		12. REPORT DATE 11 February 1977	
16. DISTRIBUTION STATEMENT (of this report) Approved for public release; distribution unlimited. Copies are available from: National Technical Information Service, Springfield, VA 22151		13. NO. OF PAGES 12 96p	
17. DISTRIBUTION STATEMENT (of the abstract entered in Block 20, if different from report)		15. SECURITY CLASS. (of this report) UNCLASSIFIED	
18. SUPPLEMENTARY NOTES		16. DECLASSIFICATION/DOWNGRADING SCHEDULE N A	
19. KEY WORDS (Continue on reverse side if necessary and identify by block number) Chemical agent detection Quadrupole mass spectrometer Field ionization mass spectrometry Silicon rubber separators Ionization sources Field induced negative ion formation Air monitoring Ambient background			
20. ABSTRACT (Continue on reverse side if necessary and identify by block number) The first phase of this project established the feasibility of using field ionization mass spectrometry for the fast detection, identification, and quantitative assessment of chemical warfare agents emitted into the atmosphere during demilitarization operations. During the second phase of the project, reported here, the objectives were to verify the sensitivity and determine the practical limits of field ionization detection of specific chemical warfare agents by a cross calibration procedure, to determine the usefulness of multiple silicon			

UNCLASSIFIED

SECURITY CLASSIFICATION OF THIS PAGE (When Data Entered)

19. KEY WORDS (Continued)

20 ABSTRACT (Continued)

rubber membrane separators for preenrichment of the analyzed air, and to search for improved field ionization sources.

Field ionization mass spectrometry was found to be an adequate technique for the detection of chemical warfare agents in pure air down to the 10 ppt level. In laboratory air, the limit is 1 ppb because of the presence of impurities. This limitation could be eliminated by prepurification of the air. Prepurification techniques involving enrichment would bring the detection limit down below the ppt (10^{-12} mole/mole) level. A new concept of field induced negative ion formation, which can be performed on the same mass spectrometric system, shows comparable sensitivity of detection of phosphonate chemical warfare agents and could be used as a corroborative procedure to diminish the probability of false alarms.

UNCLASSIFIED

SECURITY CLASSIFICATION OF THIS PAGE (When Data Entered)

PREFACE

The research described in this report was authorized under Project/Task 1T161102A71A, Basic Life Sciences Research in Support of Biological Defense Material. It was performed at Stanford Research Institute by the Mass Spectrometry Research Center under Contract No. DAAA15-73-C-0132. The technical studies in this contract were completed in June 1976.

Reproduction of this document in whole or in part is prohibited except with permission of the Commander, Edgewood Arsenal, Attn: SAREA-TS-R, Aberdeen Proving Ground, Maryland 21010; however, DDC and the National Technical Information Service are authorized to reproduce the document for U.S. Government purposes.

ACCESSION for		NTIS Section <input checked="" type="checkbox"/>
DDC		DDC Section <input type="checkbox"/>
UNANNOUNCED		
JUSTIFICATION		
BY DISTRIBUTION/AVAILABILITY CODE		
Dist.	AVAIL. and/or SPECIAL	
A		

CONTENTS

I	INTRODUCTION	9
II	TECHNICAL BACKGROUND	13
III	SENSITIVITY OF DETECTION AND CHEMICAL BACKGROUND	35
	Comparison of Single and Multiple Membrane Inlet Systems . .	36
	Field Induced Negative Ion Formation	39
IV	CROSS CALIBRATION EXPERIMENTS	43
	A. Modification of the Mass Spectrometer	43
	B. Evaluation of the Instrument, DIMP Cross Calibration . .	55
	C. Comparison of the Vapor Surveillance Quadrupole's Sensitivity to GB and DIMP	67
V	STUDIES ON FIELD IONIZATION SOURCES	73
	A. Comparison of the Field Ionization Efficiencies of the Tungsten Activated Wire Field Ionization Source with the Multipoint Array Sources	73
	B. Technique for Measuring the Natural Angular Divergence of Ions Exiting Low Intensity Ionization Sources	84
	C. Improvement of the Interfacing of Quadrupole Mass Filters with Multipoint Field Ionization Sources	86
	D. Razor Blade Sources	
VI	CONCLUSIONS AND RECOMMENDATIONS	95
	LITERATURE CITED	99
	DISTRIBUTION LIST	100

ILLUSTRATIONS

	Page
1. Field Ionization Spectrum of Diisopropyl Methanephosphonate	16
2. Field Ionization Spectrum of Diisopropylaminoethanethiol .	17
3. Field Ionization Spectrum of Bis(2-chloroethyl) Ether . . .	18
4. Field Ionization Spectrum of Bis(2-methoxyethyl) Sulfide . .	19
5. Scanning Electron Micrograph of Multipoint Field Ionizing Source	21
6. Tips of Field Ionization Source (Magnified 20,000 Times) . .	
7. Schematic Cross Section of Multipoint Source Showing Method of Introducing a Gaseous Sample	23
8. Gas Dilution and Inlet System for Field Ionization Mass Spectrometry	26
9. Sensitivity of Detection of Diisopropyl Methanephosphonate by Field Ionization Mass Spectrometry	29
10. Sensitivity of Detection of Diisopropylaminoethanethiol by Field Ionization Mass Spectrometry	31
11. Sensitivity of Detection of Bis(2-chloroethyl) Ether by Field Ionization Mass Spectrometry	32
12. Sensitivity of Detection of Bis(2-methoxyethyl) Sulfide in Air by Field Ionization Mass Spectrometry	33
13. Double Membrane Inlet System	38
14. Negative Ion Spectrum of DIMP	40
15. Bottom View of Multipoint Field Ionization Source	44
16. Schematic of the Field Ionization Vapor Surveillance Quadrupole Instrument	47
17. Ionizer High Voltage Power Supply Input Regulator Circuit .	48
18. Grid Voltage	40
19. Quadrupole Drift over Time	52

ILLUSTRATIONS (Concluded)

	Page
20. System Pressure Versus Gauge Indication, Edgewood Quadrupole	53
21. Sample Inlet Flow System	57
22. Sensitivity Measurement with Xylene	59
23. Sensitivity Measurement with Bis(2-chloroethyl) Ether	60
24. Sensitivity Measurement with DIMP	61
25. Sensitivity Measurement with Xylene before Shipment of Instrument	64
26. Sensitivity Measurement with DIMP under Continuous Input	66
27. Sensitivity Measurement with DIMP at Edgewood Arsenal	69
28. Sensitivity Measurement of GB at Edgewood Arsenal	70
29. Test Arrangement for Multipoint Sources	76
30. Test Arrangement for Activated Wire Source	77
31. Schematic of Test Mass Spectrometer	78
32. Schematic of Sample Feed System	80
33. Schematic of the Apparatus Used to Determine the Angular Divergence of Ions Exiting an Ion Source	85
34. Two Interfacings of Field Ionization Source with Quadrupole Analyzer	90
35. Mass Analyzed Count Rate Versus Decelerator Entrance Voltage	92
36. Razor Blade Slit-Type Ionization Source	93

TABLES

	Page
1. Sensitivity Requirements for Real Time Monitors for Demil Plant Effluents	14
2. Response of Instrument to Simulants	27
3. Relative Efficiencies of Multipoint FI Sources and Activated Wire Emitters	82
4. Envelope Divergence Half Angle for Ions Emitted from Multipoint FI Sources	87

I INTRODUCTION

The objective of this research was to evaluate the potential use of field ionization mass spectrometry (FIMS) for the "real time" detection of chemical warfare (CW) agents, specifically GB and VX, in air at concentrations from 0.001 to 1 ppb (mole/mole). Monitoring of these agents in air in this concentration range is required to ensure the safety of incineration of CW munitions as part of the demilitarization (Demil) program. Following establishment of the feasibility of the concept, under Contract DAAA15-74-C-0103, we undertook the present phase of research under Contract DAAA15-75-0132. The tasks of this phase of research were to:

1. Corroborate the preliminary findings on the sensitivity of FIMS to detect CW agents in air and determine the practical limit of their detection.
2. Cross calibrate the efficiency of detection of GB by FIMS with that of diisopropyl methyl phosphonate (DIMP) used as a simulant. These tests were performed at Edgewood Arsenal because of the prohibition on the transport and use of GB.
3. Determine the efficacy of multiple silicon rubber membrane separators for preenrichment of the analyzed air.
4. Search for improved field ionization sources, since the existing multipoint sources exhibit limited durability on constant feed with air.

The preliminary results on the sensitivity of FIMS to detect CW simulants have been completely corroborated, and a limit of detection of 10 ppt of DIMP in pure air has been established using a single silicon rubber membrane. This sensitivity is, however, 100 times higher than the practical limit of 1 ppb because of impurities in the laboratory air (and most probably in the air emitting an incinerator).

Cross calibration experiments required the adaptation of a transportable quadrupole mass spectrometer, belonging to Edgewood Arsenal, with an FI source. The tests performed at Edgewood showed that the sensitivity of detection of GB is somewhat higher than that of DIMP. Thus, the simulation studies on DIMP carried out at SRI are directly applicable to the detection of CW agents.

The comparison of single, double, and triple silicon rubber membrane air separators showed no substantial increase in sensitivity with the multiple membrane systems, although the double membrane allows more effective control of the ionization source pressure. The double and triple membranes, however, show extremely long response times to a signal of DIMP. Although this time lag is somewhat shorter with GB, as was shown in the experiments at Edgewood, it contra-indicates the use of a triple membrane and strongly suggests the use of a single membrane with an adsorptive pre-enrichment system.

Comparisons of the field ionization efficiencies of the Beckey type preconditioned tungsten wire FI source and the SRI multipoint source showed that the multipoint source is about two orders of magnitude more efficient. This makes the wire source rather unattractive. A new slit type activated edge field ionization source was developed and tested. The preliminary results are sufficiently encouraging to strongly suggest a continued development effort.

SRI's new concept of ionization, "inverse" field ionization or field-induced negative ion formation (FINIF), has been tested on CW simulants with encouraging results. The characteristic fragment ions PO_2^- and PO_3^- that were detected allowed detection sensitivities of 1 ppb. After interfering impurities are removed, these ions may facilitate the detection of 50 ppt concentration of phosphorus-containing CW agents in air. Further work on this mode of ionization is therefore strongly indicated.

In conclusion, it has been shown that FIMS is an adequate method for the "real time" detection of CW agents in air down to 1 ppb level, and that the detection is limited by the presence of trace impurities in air, which might be removed by preadsorptive separation. Removal of impurities could increase the sensitivity by at least three orders of magnitude. The use of FINIF to corroborate the presence of phosphonic CW agents in air, which can be readily performed on the same mass spectrometric system, is a highly powerful tool to reduce false alarms.

II TECHNICAL BACKGROUND

The fast detection and identification of trace amounts of chemical warfare agents is essential for efficient and safe disposal schemes. The maximum permissible concentrations of these materials in the atmosphere are given in Table 1. The most toxic of these materials, VX, has a molecular weight of 267; therefore, the molar concentrations we are dealing with are of the order of 10^{-15} moles/liter in the most extreme case. The real-time requirement (defined here as response within 60 seconds) for effective monitoring precludes elaborate concentration processes, and if the analysis is carried out in, say, 1 milliliter of air, we are confronted with the problem of detecting 10^{-15} moles, or 6×10^8 molecules in all. The only analytical procedure capable of quantitative assessment of such small numbers of molecules is mass spectrometry.

Classical mass spectrometry using electron impact for ionization can have a fairly high ionization efficiency (of the order of 10^{-4}), but the ionization produces extensive fragmentation. For example, the electron impact ionization of malathion (which is chemically related to some chemical warfare agents) results in a yield of 0.3% of the parent ion (mass 330) and 99.7% of ionic fragments scattered from mass 16 to 330 with predominant masses of 93, 99, 125, 128, 145, 158, 173, and 285.¹ This extensive fragmentation not only reduces the sensitivity of detection to an impractical level, but precludes any meaningful analysis of air without pre-separation because the complex fragmentation pattern of other impurities in air will obscure the spectrum of the desired material beyond recognition.

Table 1. Sensitivity Requirements for Real Time Monitors for Demil Plant Effluents

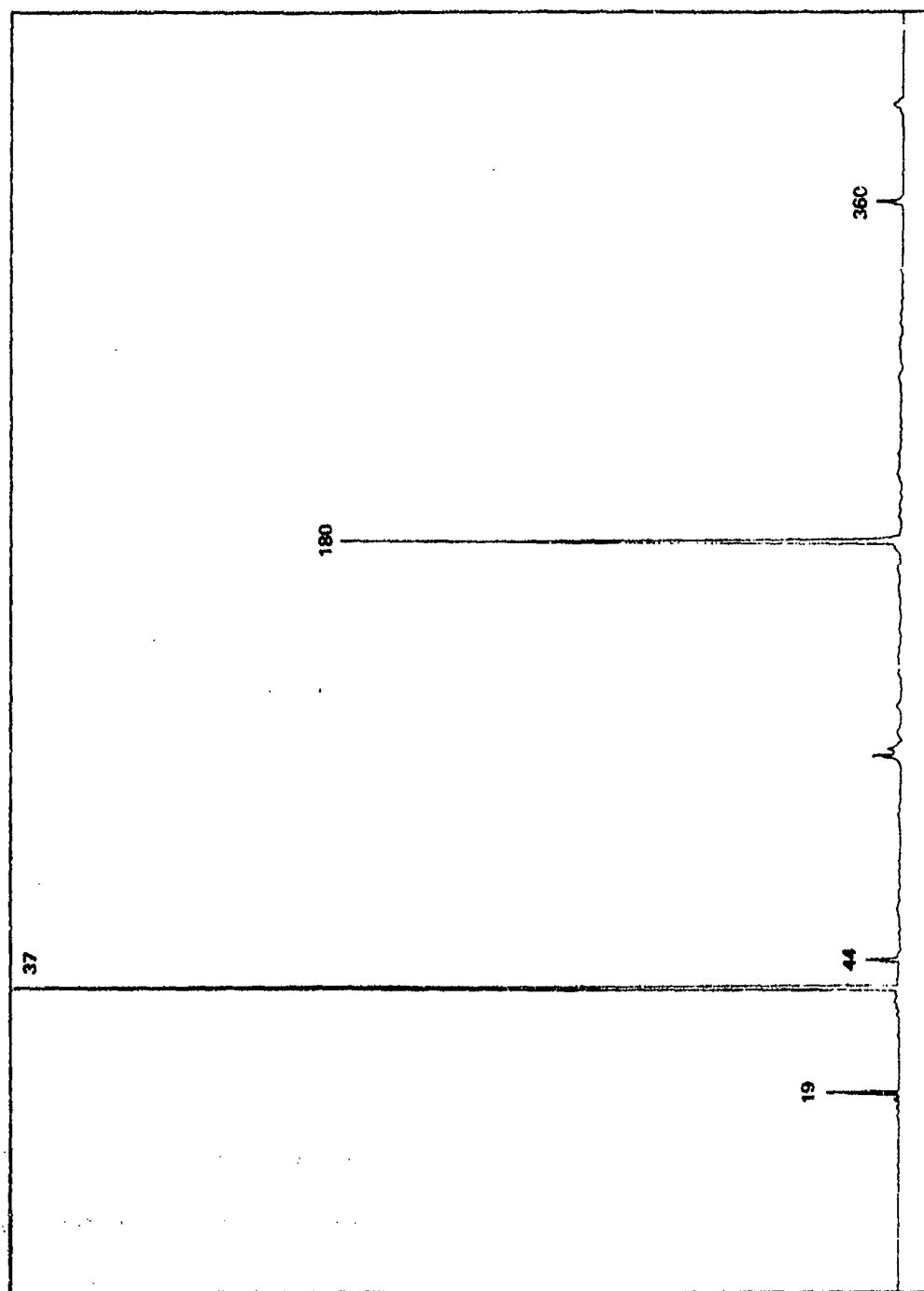
Effluent	Maximum allowable concentrations			
	grams/liter	molecules/cm ³	mole fraction	
GB	Stack	3 x 10 ⁻¹⁰	1.3 x 10 ⁹	5.1 x 10 ⁻¹¹
	Working area	1 x 10 ⁻¹⁰	4.4 x 10 ⁸	1.7 x 10 ⁻¹¹
	Perimeter	3 x 10 ⁻¹²	1.3 x 10 ⁷	5.1 x 10 ⁻¹³
VX	Stack	3 x 10 ⁻¹¹	6.9 x 10 ⁷	2.7 x 10 ⁻¹²
	Working area	1 x 10 ⁻¹¹	2.3 x 10 ⁷	9.1 x 10 ⁻¹³
	Perimeter	3 x 10 ⁻¹³	6.8 x 10 ⁵	2.7 x 10 ⁻¹⁴
HD	Stack	3 x 10 ⁻⁸	1.1 x 10 ¹¹	4.5 x 10 ⁻⁹
	Working area	1 x 10 ⁻⁹	3.8 x 10 ⁹	1.5 x 10 ⁻¹⁰

Other modes of ionization induce much less fragmentation than electron impact. The best in this respect is field ionization, which for malathion results in over 60% parent peak formation, and for parathion, sumthion, methyl parathion, paraoxon, and diazinon yields more than 90% parent ions.¹ Commercially available field ionization sources,² however, are inefficient and have a rather short useful lifetime.

Field ionization utilizes strong electric fields (approximately 10 volts/Å), which are obtainable with needle points, fine wires, and razor blade edges. These strong fields permit the outer molecular electrons to tunnel through and escape the potential barrier of the molecule, thus producing positive ions.³ This ionization process is gentle and provides the molecule with the minimum energy necessary to extract the loosest bound electron. The nonfragmenting nature of FIMS is exemplified in figures 1 through 4, taken from the previous report.

SRI has developed a porous field ionization source that is currently about two orders of magnitude more effective than the ones previously available.⁴ At this stage of development, we have achieved an ionizing efficiency of 10^{-4} and a mass selection efficiency of 10^{-3} . Even with an overall detection efficiency of 10^{-7} , air containing one part in 10^{12} malathion will give 1.0 count/min at the parent ion without pretreatment. Following passage through a single silicon rubber membrane, the counting rate increases to over 100 counts/min. As we showed in the report on the first phase of this project,⁵ comparable sensitivity has been demonstrated for the simulants tested in this project.

By virtue of its nonfragmenting nature, FIMS is ideally suited for the analysis of complex mixtures such as the analysis of polluted air. With proper calibration of the mass spectrometer for ionization and detection efficiency for the different species, the components of the mixture can be measured reproducibly with a high precision.⁴ The ionization



SA-3122-6

Figure 1. Field Ionization Spectrum of Diisopropyl Methanephosphonate (M.W. 180)

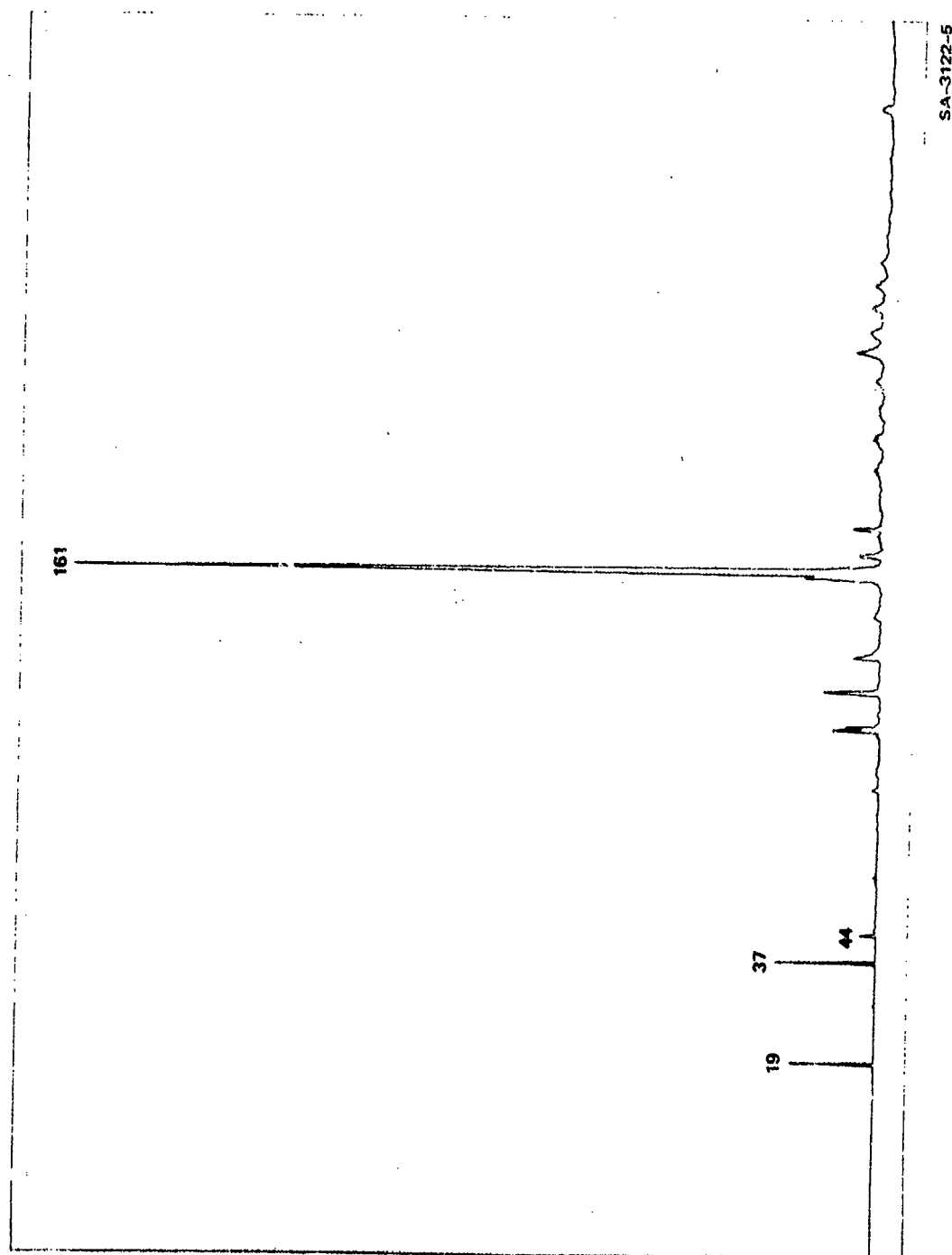
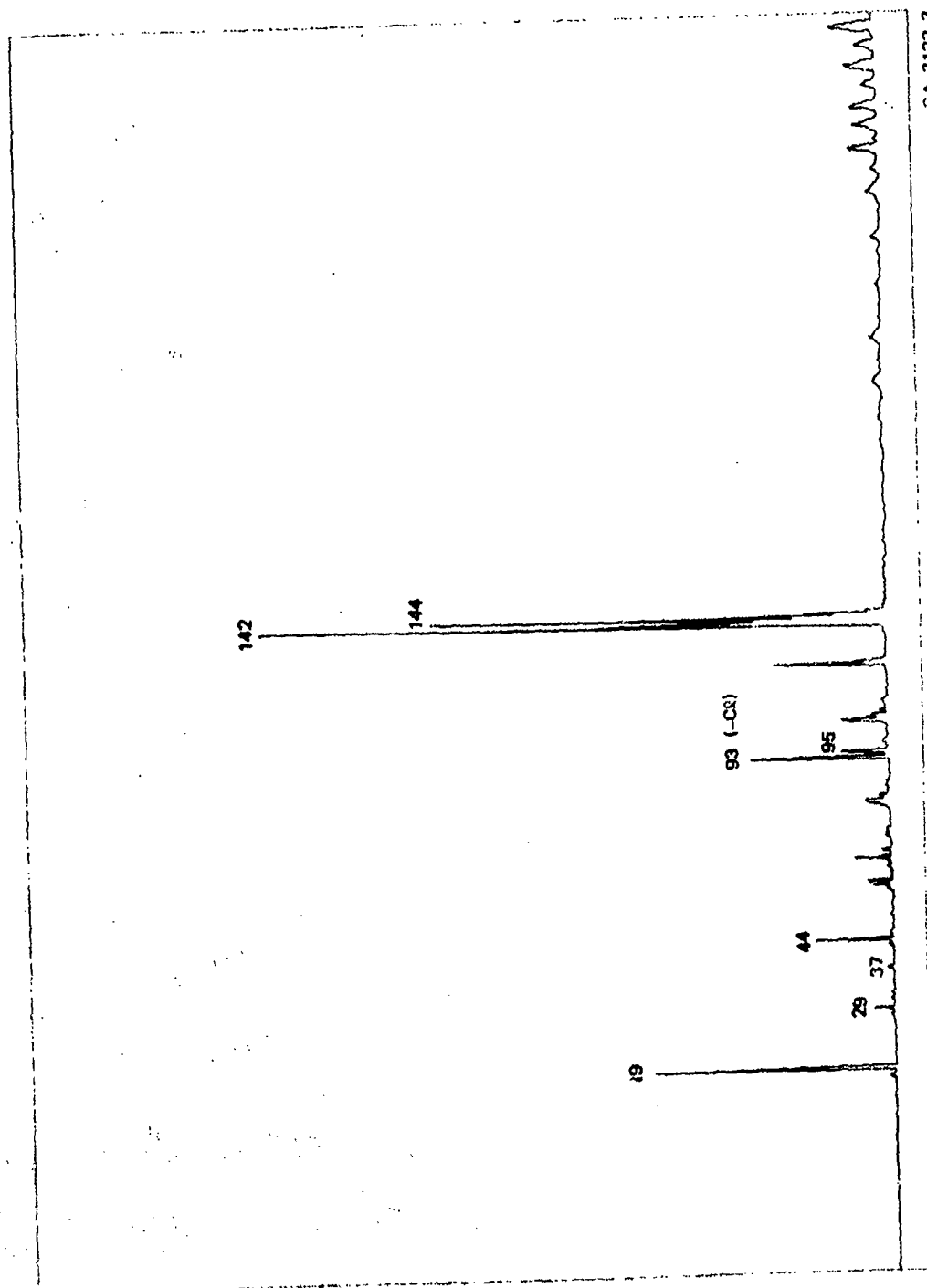
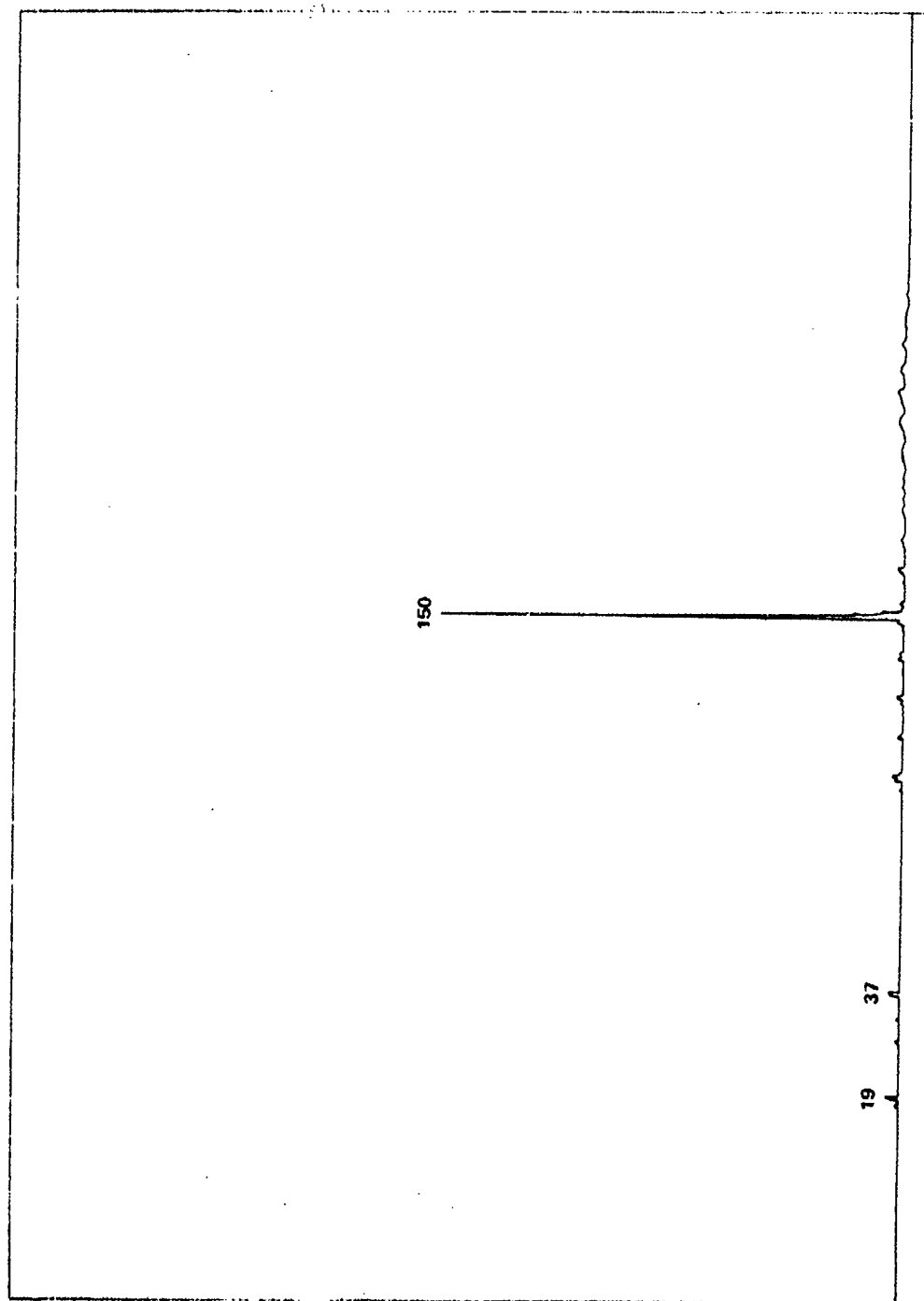


Figure 2. Field Ionization Spectrum of Diisopropylaminoethanethiol (M.E. 161)



SA-3122-3

Figure 3. Field Ionization Spectrum of Bis(2-Chloroethyl) Ether (M.W. 142, 144)



SA-3122-4

Figure 4. Field Ionization Spectrum of Bis(2-Methoxyethyl) Sulfide (M.W. 150)

efficiency by field ionization of different organic species is the same within a factor of two irrespective of the chemical nature of the analyzed material.

As stated above, field ionization is facilitated by the high field gradient that can be produced at surfaces with very high curvatures. A cathode with a radius of curvature of about 0.1 micrometers (μm) and an anode at a distance of 25 μm require less than 1000 volts to produce field ionization. Such a configuration is readily attainable in a reproducible manner by the appropriate technology.

SRI developed the technology for producing arrays of hundreds of microcones on a porous substrate.⁶ These arrays constitute the crucial element in our present ionization sources. They allow better sample feed and more uniform and reproducible operation than the field ionization sources previously used. Figure 5 shows such a structure mounted on a screen, and figure 6 is a scanning electron micrograph of one of the tips. Figure 7 shows the cross section of an operational field ionization source in which the temperature of the sample inlet can be controlled independently of the temperature of the source. The temperature of the source is constant and higher than the maximum temperature the sample is subjected to; this prevents memory effects and results in more controlled ionization conditions.

We have examined the effect of dilution with air on the efficiency of ionization of organic molecules.⁷ We diluted toluene with air down to 20 ppm without any significant loss in ionization efficiency, which was about 10^{-4} in this particular case. This result shows that air does not interfere with the ionization process of minor constituents, even if present in minute quantities. In an analogous experiment, toluene was diluted in methanol down to 1:1000, again without change in its ionization efficiency. A similar result was obtained when

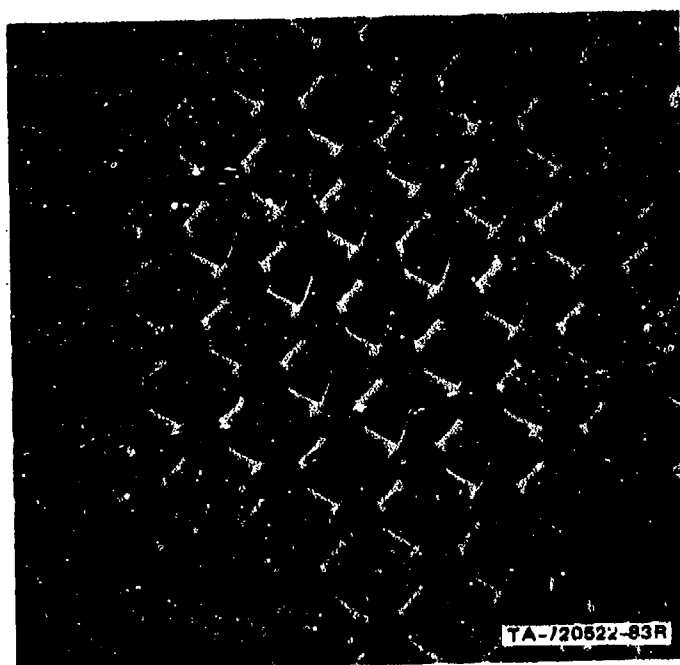


Figure 5. Scanning Electron Micrograph
of Multipoint Field Ionizing Source



1 μ

Figure 6. Tips on Field Ionization Source
Magnified 20,000 Times

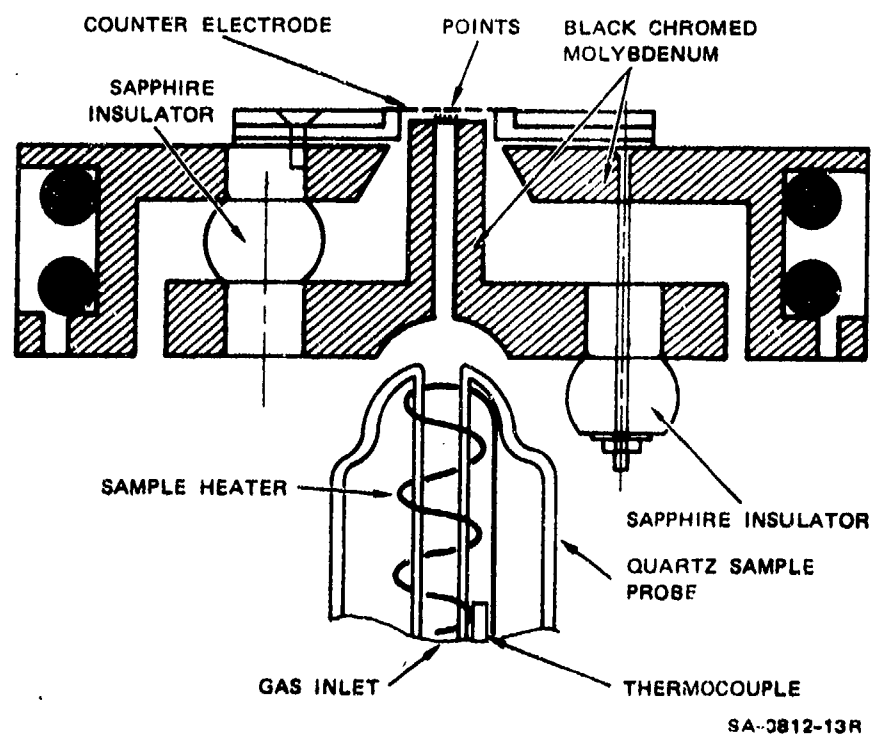


Figure 7. Schematic Cross Section of Multipoint Source Showing Method of Introducing a Gaseous Sample

methanol was diluted with toluene down to 1:1000. Again, the ionization efficiency of methanol remained constant and equal to that of pure methanol.

Thus our ionization source seems to be able to ionize minor constituents of a mixture containing dissimilar chemicals without significant changes in the individual efficiencies of ionization. This result was corroborated for a number of simulants of chemical warfare agents, as discussed in the previous report.⁵

We have found that a magnetic sector momentum analyzer is best suited for this project. This instrument was used in the feasibility study. The magnetic sector analyzer gives us the option of accelerating voltage scanning over a limited mass range or magnetic scanning using a precise fast responding magnetometer for the real-time determination of the magnetic field. Magnetic scanning has the advantage of fixed geometry and less likelihood of change of transmission with mass, whereas accelerating voltage scanning has a faster response and may be simpler to install. Compared with the quadrupole analyzer, the magnetic sector has a higher ion transmittance when analyzing the highly divergent high energy ions emitted from a field ionization source. The high transmittance efficiency is critical when ultra-high sensitivity is required for the monitoring system, as is the case in the present application.

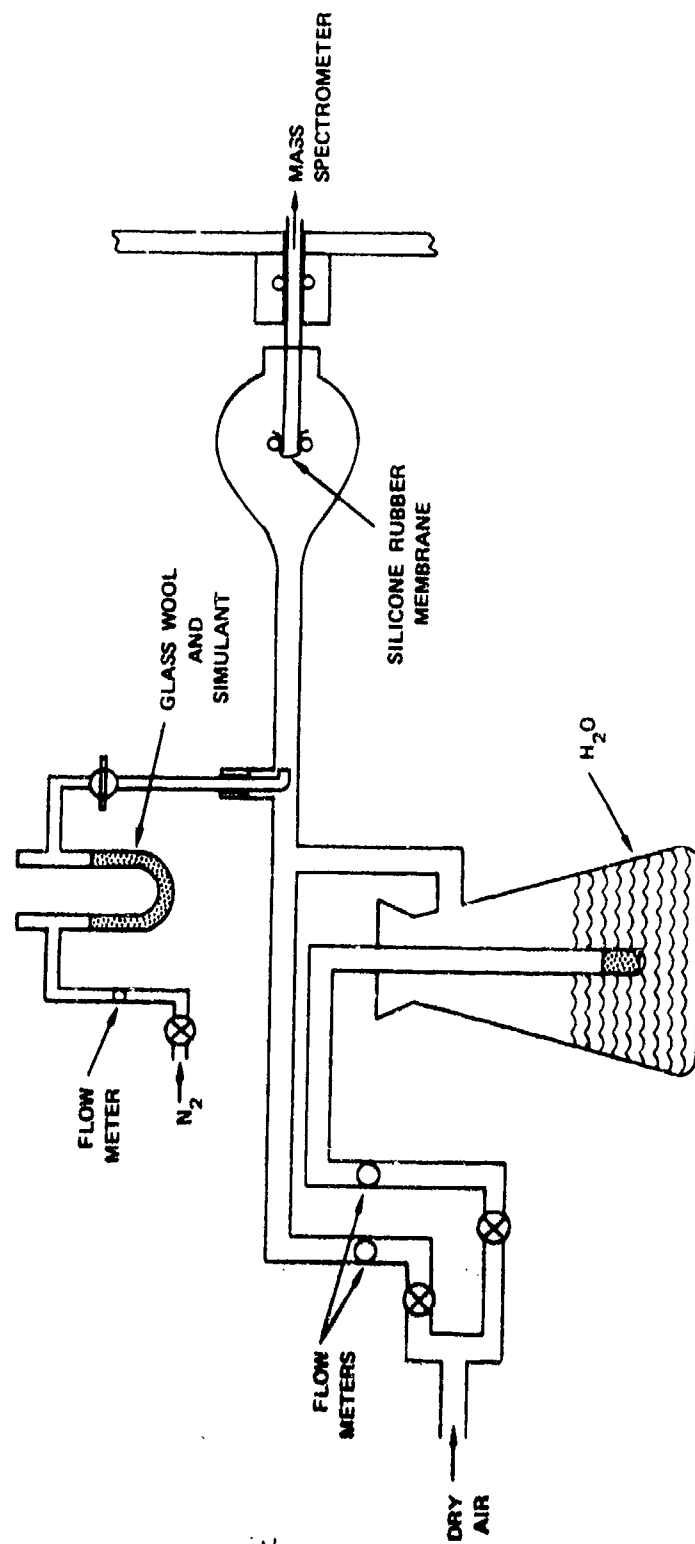
In view of these considerations, we carried out our preliminary experiments on our 45° magnetic sector field ionization mass spectrometer, which has only recently been adapted to operate in a multi-scanning mode by modulation of the accelerating voltage. This instrument is far from ideal for this purpose because it was designed for high dispersion and low resolution. Still, it provides us with reliable, reproducible information on the detection sensitivity of chemical

agents in the atmosphere. This information is necessary for the design of a special-purpose monitor of CW agents or their products in the effluents from a demilitarizing plant.

The sampling and inlet system used in the first phase of the project is described in figure 8. The chemical agent simulant to be tested was placed on glass wool in a U-tube, and dry nitrogen was passed through it to generate a stream saturated in simulant at room temperature. The simulant stream was combined with a stream of air of controlled humidity to give the final concentration. The final air stream was passed through an expansion volume containing the membrane inlet system to the field ionization source. The membrane inlet consists of a disc of dimethyl silicon rubber (1-mil thick) covering a fine mesh screen that is cemented to the end of a capillary glass tube. The capillary has a 0.8-mm I.D. and a 6-mm O.D. The tube leads through an O-ring seal to the field ionizer. The effective areas of membrane tested were 1 or 2 mm². The pressure rise above background, resulting from the passage of atmospheric gases into the source region, was about 2×10^{-7} torr. This pressure increased slightly with increased humidity. The inlet system was operated at room temperature.

The ionizer was operated at 100°C and at a field strength sufficient to produce a plateau of ion counts at the detector for low levels of simulant. Field strength ranged from 1 to 3 kilovolts (kV), depending on the ease of ionization.

The experimental results obtained in the first phase are summarized as follows. The response of the detection was linear, with concentration up to the limit of counting equipment for all four simulants of CW agents tested in this phase: DIMP, diisopropylaminoethanethiol (DIAET), bis(2-chloroethyl) ether (BCEE), and bis(2-methoxyethyl) sulfide (BMES). The results are summarized in table 2. Response was also proportional to the area of the silicon rubber membrane exposed.



SA-3122-2

Figure 8. Gas Dilution and Inlet System for Field Ionization Mass Spectrometer

Table 2. Response of Instrument to Simulants

Compound	Molecular weight	Vapor pressure at 24°C (torr)	Source Material	Sensitivity *	
				ppb	g/liter
DIMP	180	0.27	Cu	1.3×10^{-1}	9.6×10^{-10}
DIAET	161	0.02	Cu	1.0×10^{-1}	6.6×10^{-10}
BCEE	142, 144	1.1	Cr/Cu	8.0×10^{-1}	4.7×10^{-9}
BMES	150	0.25	Cr/Cu	1.7×10^{-1}	1.1×10^{-9}

* In dry air to give 1000 counts/min. In all cases, increased humidity increased sensitivity 5% to 15%. Signal-to-noise ratio was 5:1 in laboratory air.

The response of the room temperature inlet system to DIMP was quite slow. A high concentration (> 50 ppb mole ratio) reached a constant count rate in about 10 minutes. At lower concentrations, the time required to reach a constant response grew longer, requiring 30 minutes to respond to 5 ppb. This delay is presumably the time it takes DIMP to reach the ionizing region of the source by way of the long capillary glass inlet and metallic source design. Raising the temperature of the inlet system to 80°C decreased the response time by more than a factor of 50. The sensitivity of detection was enhanced by the pressure of water vapor. At 30% relative humidity (RH), the count rate increased by 20%, indicating that swelling of the membrane in the presence of moisture permitted faster transport of the DIMP molecules. The limiting sensitivity of the system using the 0.8-mm bore capillary and $\sim 1\text{-mm}^2$ membrane in the flowing dry air stream was about 1 ppb for the signal-to-noise ratio of 1 (figure 9).

The response to DIAET was more effective than to DIMP. These molecules are very easily ionized, which lowers the noise figures at the measured mass. The response was again slow to reach a plateau, partly because of the very low levels of simulant needed. Typically, 15 minutes were needed for a steady-state detection at 40 ppb. Again, this response time was reduced to seconds when the inlet system was heated to about 100°C . Water vapor slightly increased the signal level; at 30% RH, the signal was about 5% above the 0% RH level.

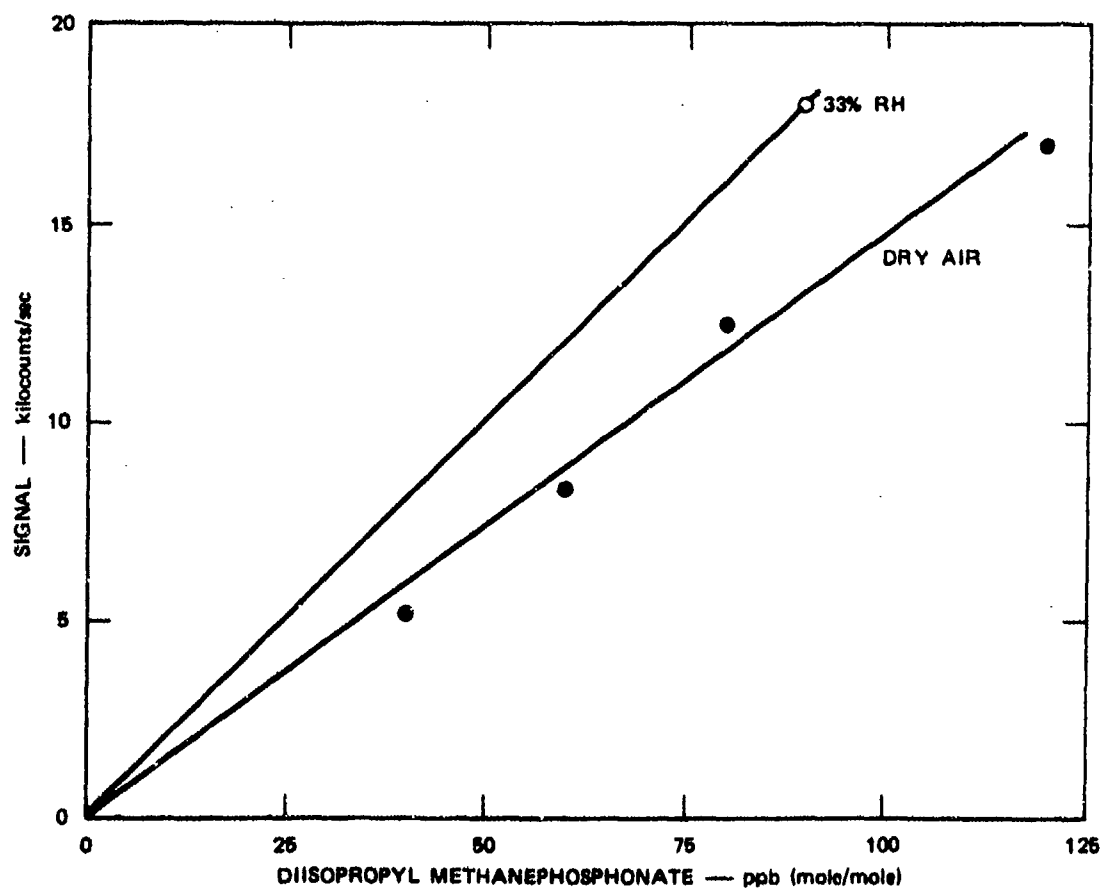


Figure 9. Sensitivity of Detection of Diisopropyl Methanephosphonate by Field Ionization Mass Spectrometry

Detection sensitivity for DIAET was about 0.1 ppb for a signal-to-noise ratio of 5 with the 1-mm² membrane (figure 10). The concentration of the simulant was not verified chemically, and the white deposit that formed on the glassware of the simulant gas stream indicated some loss of simulant to the walls. Thus the sensitivity of detection calculated for vapor pressure is a conservative estimate. We used the vapor pressure data as measured by a McLeod gauge, namely, 50 millitorr at 40°C.

BCEE proved to be more difficult to detect. The chlorinated ions react with the copper used in the construction of the field ionizing source. This reaction results in a deterioration of the signal with time, particularly in the presence of water vapor. This shortcoming was later overcome by substituting chromium-plated copper tips for the original copper tips. Chromium-plated tips have been shown to operate continuously for many days without any significant decline in ionization efficiency.

The molecule of BCEE is relatively difficult to ionize, requiring 4.5 kV compared with 2 kV for DIAET. However, the response of the system to BCEE is very rapid, requiring only seconds to produce a stable signal. In dry air the system can detect a level of about 1 ppb at a signal-to-noise ratio of 5 (figure 11). In moist air (RH = 6%), however, the signal dropped to 1/3, giving an extrapolated detection concentration of ~ 10 ppb. The new chromium-plated source showed, however, no deterioration in sensitivity in the presence of moisture.

Another simulant of mustard gas (BMES) shows an ionization efficiency comparable to that of DIMP (figure 12), giving a sensitivity of detection better than 0.2 ppb for a single 1-mm membrane. The sensitivity of detection of mustard gas under the same condition is expected, therefore, to be somewhere between 0.2 and 10 ppb. A closer estimate could not be obtained without a measurement of the authentic material.

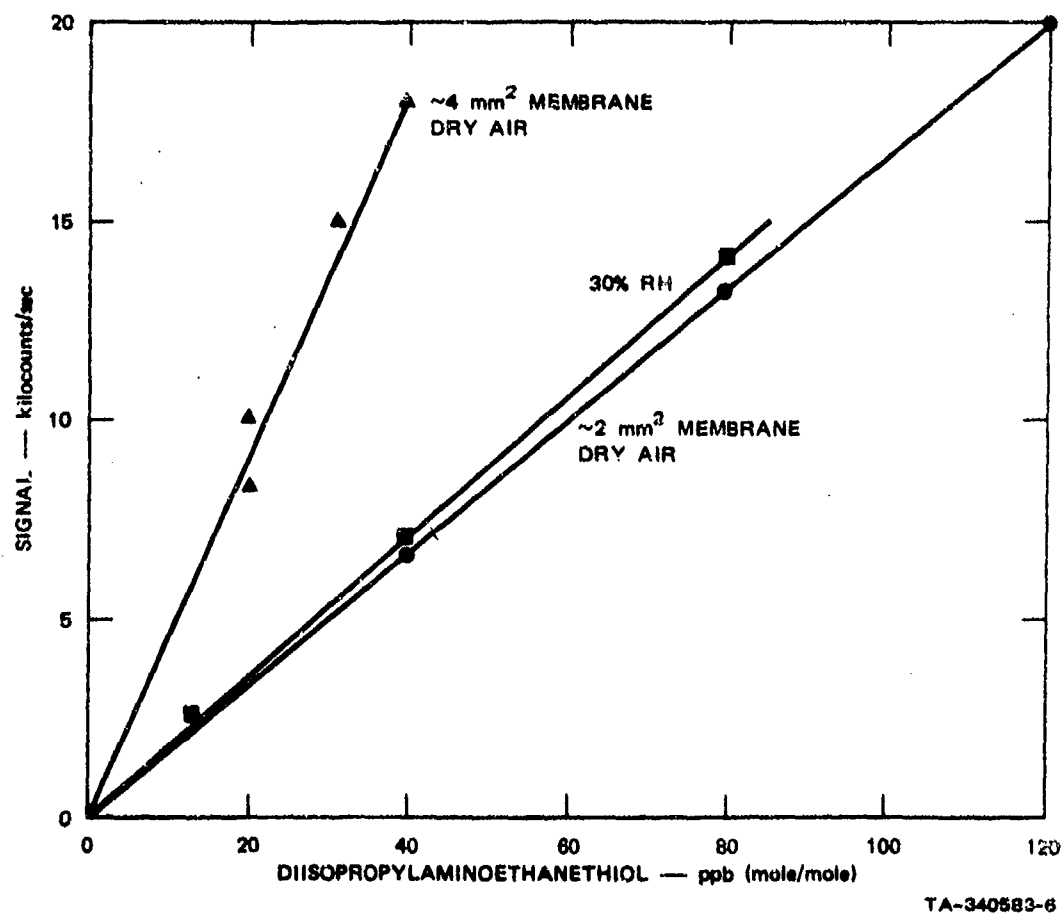
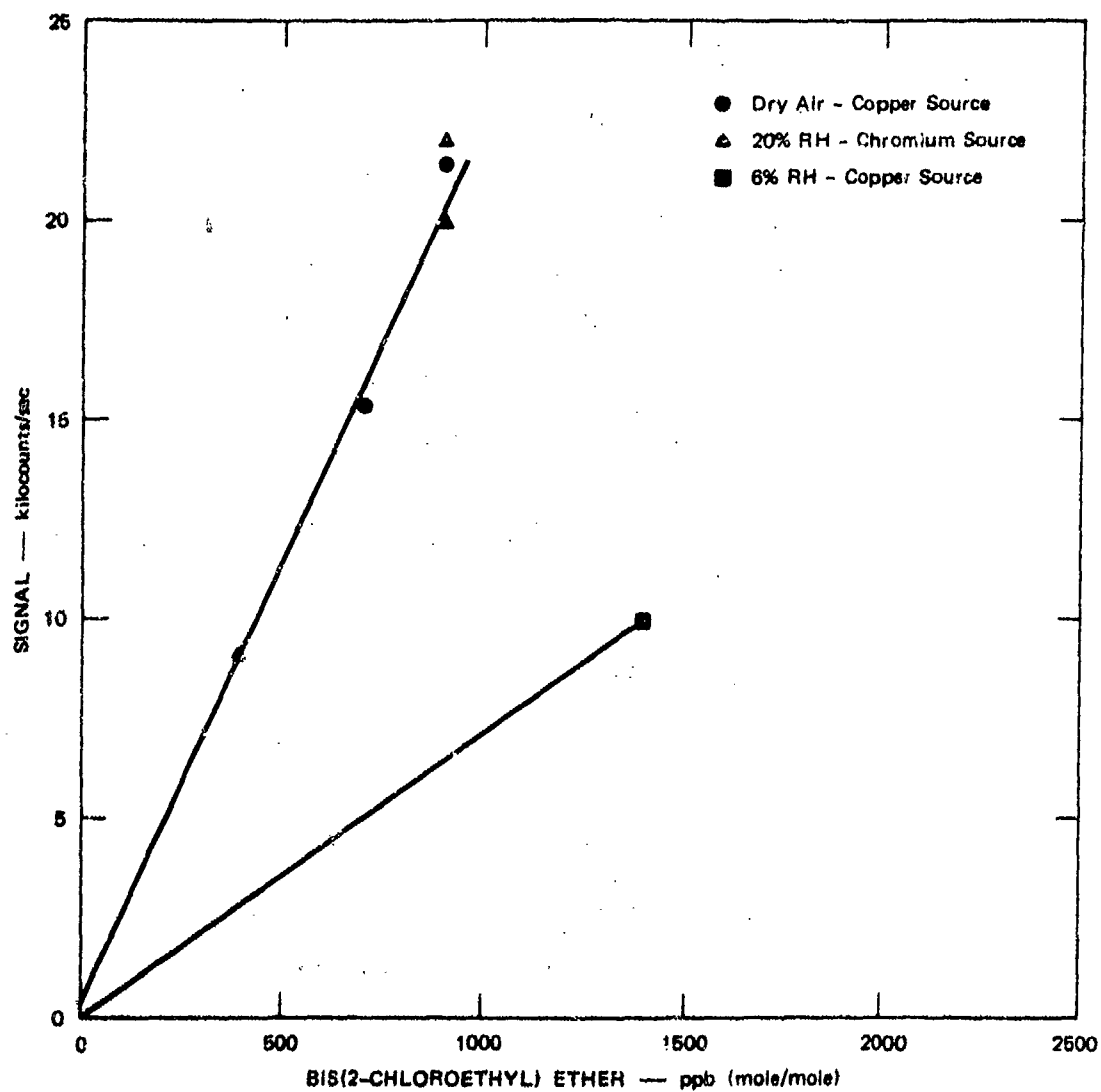


Figure 10. Sensitivity of Detection of Diisopropylaminoethanethiol by Field Ionization Mass Spectrometry



TA-340583-7

Figure 11. Sensitivity of Detection of Bis(2-Chloroethyl) Ether by Field Ionization Mass Spectrometry

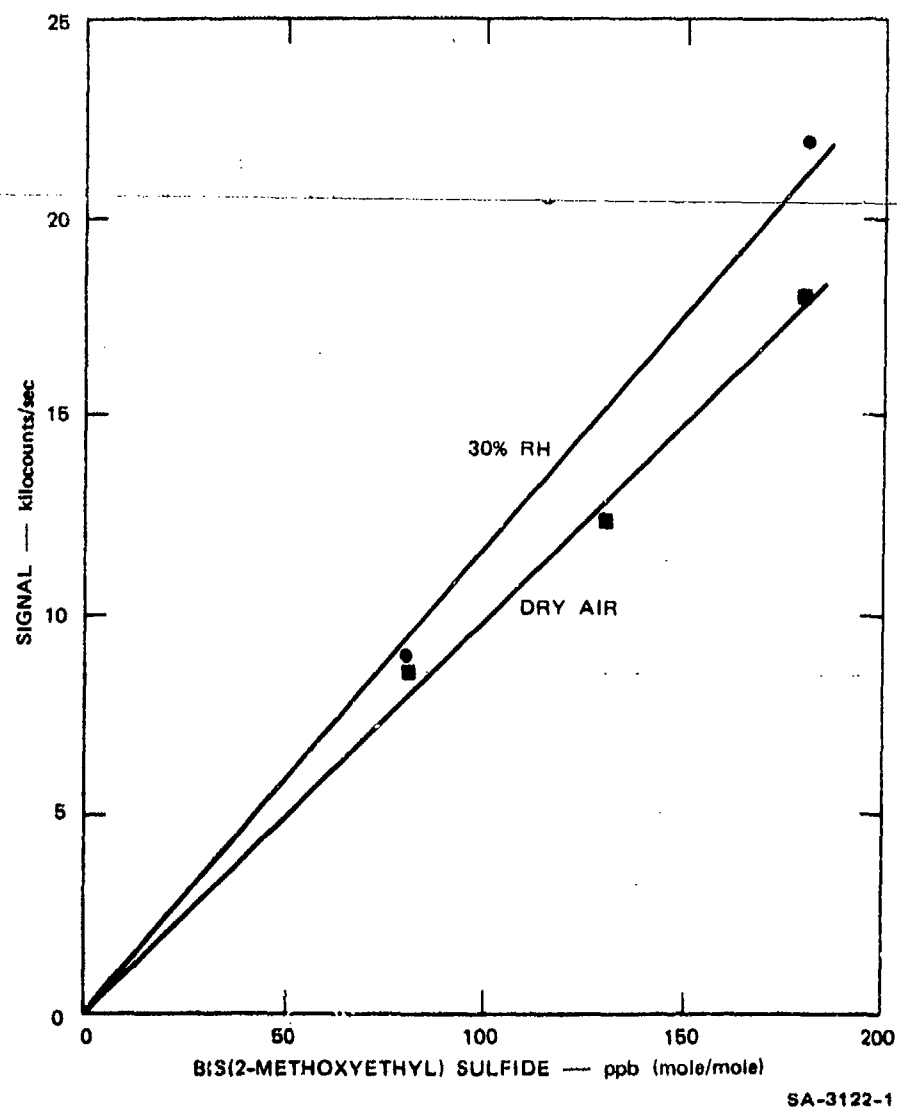


Figure 12. Sensitivity of Detection of Bis(2-Methoxyethyl) Sulfide in Air by Field Ionization Mass Spectrometry

III SENSITIVITY OF DETECTION AND CHEMICAL BACKGROUND

In the current phase of the program, we repeated the measurements of DIMP in air with modified multipoint ionization sources (closer spacings of point-to-grid and lower operating voltages). The 45° magnetic sector mass spectrometer was used as the standard instrument for testing the inlet and ionization configurations developed under this program. The field ionization source consisted of a 1.0-mm circular array of chromium-coated copper points spaced at the intersections of a 1000-mesh copper screen. The gas phase sample was fed to this multipoint array from the back by means of a heated glass inlet probe. The probe and the back of the source were ground to the same curvature for effective mating.

The sensitivity measurements of DIMP in air passed through a single or double silicon-rubber-membrane showed linear response over the range 40 ppb to 120 ppb and corroborated our preliminary findings in that we obtained 150 to 170 counts/sec/ppb of DIMP. Since an electronic and instrumental background of 1 count/sec can be achieved, DIMP concentrations in air down to 10 ppt can be detected with the present field ionization sources and mass analyzers, within 2 to 3 minutes.

In later tests, we also monitored the peaks adjacent to DIMP. These tests showed a "chemical" background of about 200 counts/sec at each amu in the range 170 to 190 amu. This background, which is 100 times higher than the noise between peaks, puts a limit on the detectability of DIMP in laboratory air at 1 ppb. We monitored the laboratory air without any DIMP present to determine the actual background at mass 180 (the molecular weight of DIMP). A background of about 150 counts/sec was found. A comparable background of 100 to 160 counts/sec was also found for the mass range 135 to 155, which covers the molecular weight of GB.

It seems likely that the sensitivity of detection of these agents will be limited primarily by "chemical" background, rather than by the sensitivity of the mass spectrometric instrumentation.

Comparison of Single and Multiple Membrane Inlet Systems

The sensitivity of the magnetic sector mass spectrometer was determined when used with a 4-mm² single membrane inlet, a ~ 400-mm² double membrane inlet, and the Varian triple inlet. Generally, the addition of one or two additional membranes increased the ease of controlling sample feed to the ionizer of the mass spectrometer, but the sensitivity of detection at a given sample inlet pressure was no higher than with a single membrane. All the enhancement of simulant over background gases occurred at the first membrane. Multiple membranes allowed use of larger areas of membrane and freedom to control the amount of gas load at the source, excess sample being discarded in the membrane cavity.

The counts/sec/ppb measured for the three membrane inlet systems are given below.

	<u>Single Membrane</u>	<u>Double Membrane</u>	<u>Triple Membrane</u>
DIMP	150	170	150
Bis(2-chloroethyl) ether	20	30	50

Both the Varian membrane unit and our double-membrane unit were very slow to reach an equilibrium signal level when DIMP was used; four or more hours were required to obtain a satisfactorily steady signal.

The metal surfaces in which the double-membrane holder came in contact with the sample were then Teflon lined. Using this modification of the holder, we lowered the response time to 1-2 hours, but this is

still an impractical response time. (The same inlet has a response time of less than 5 seconds for hydrocarbons like xylene.) The enormous difference in behavior of the two groups of chemicals is the extremely effective adsorption of the phosphonates on surfaces, metal surfaces in particular; until these are saturated, the rate of effusion of DIMP through the ionizing grid will be significantly lower than the rate of intake through the membrane.

We experienced additional difficulties in using the Varian triple membrane inlet with our field ionization mass spectrometer. The two internal cavities require separate needle control valves and should have separate pressure measuring sensors to optimize the transfer of the desired atmospheric constituent reaching the ionizer. Heating the inlet slightly lowered the response time, but aggravated the problems of pressure control since the silicon membranes transmitted a higher proportion of undesired constituents, resulting in a lower enrichment factor.

To try to solve the dual problems of pressure control and slow response time, we redesigned our double membrane inlet so that it could be closely coupled to the field ionizer. The metal parts were coated with Teflon to minimize adsorption on surfaces of the inlet. The active area of the membranes was 4.5 cm^2 . The silicon rubber was backed with 100-mesh etched screen supported on 40-mesh woven stainless screen. The backing screens were not Teflon coated.

Figure 13 shows the double membrane inlet attached to the field ionization source and lens system. The sample air stream passes through the vacuum flange in 6-mm stainless tubing, enters the membrane holder where components are separated from the air, and returns to the flow-controlling valve outside the vacuum system through the exhaust 6-mm stainless tube. The separated components diffuse into the intermediate

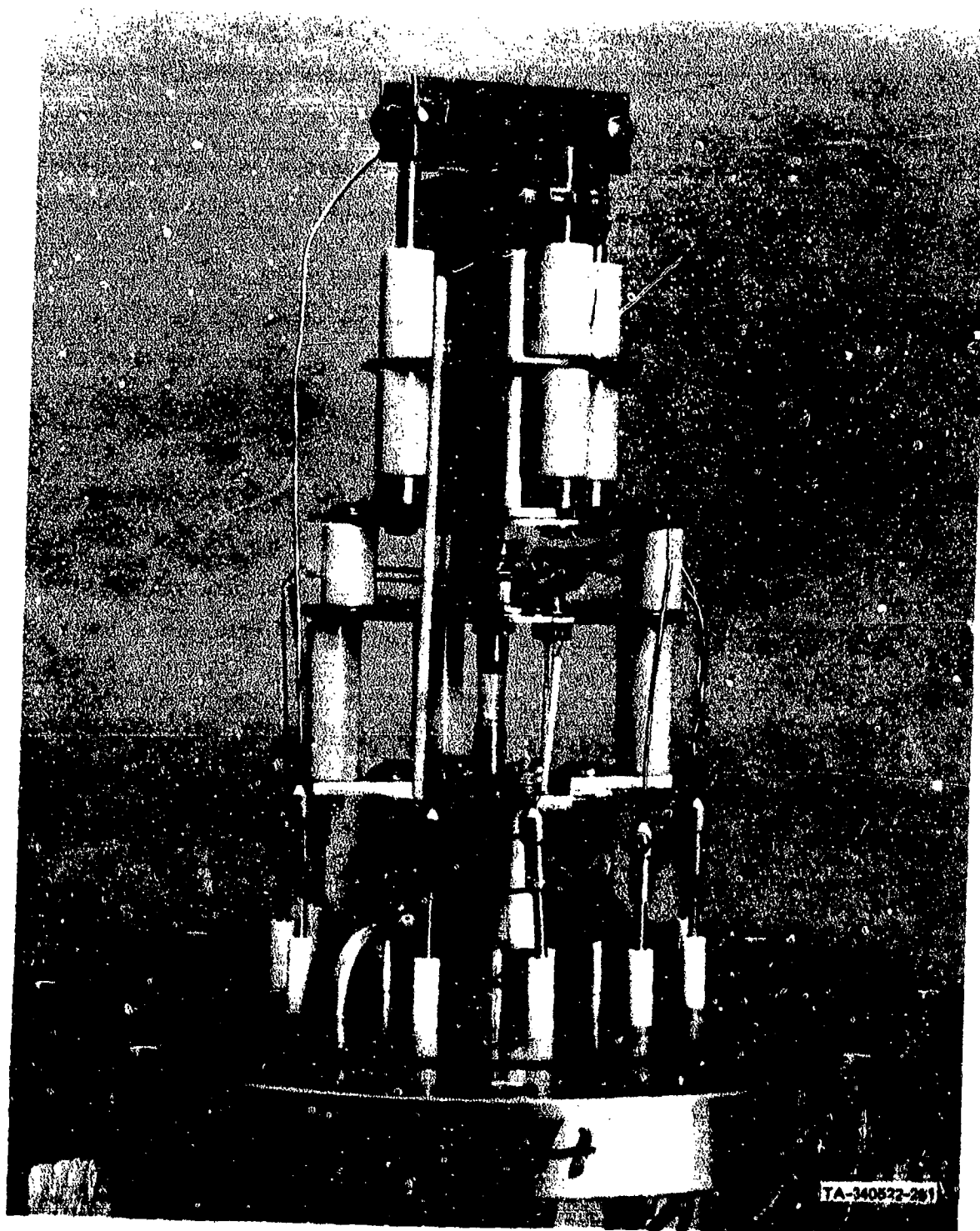


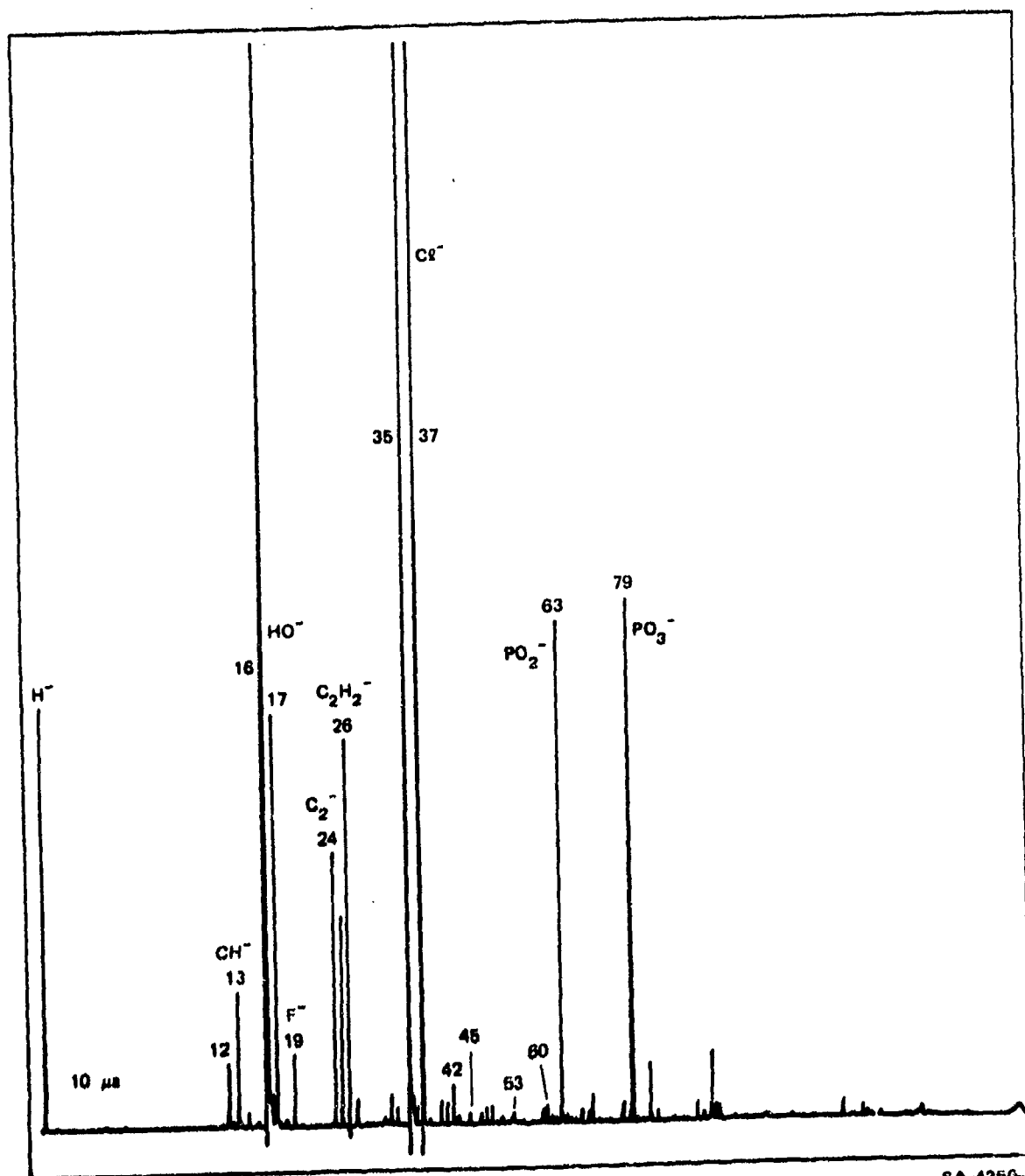
Figure 13. Double Membrane Inlet System

volume of the membrane inlet where the pressure is controlled externally by a needle valve and vacuum pump acting through a third 6-mm stainless tube passing through the vacuum flange. The sample then diffuses through the second membrane and enters the high vacuum through the field ionizer. The membrane inlet and the ionizer are electrically isolated, since a potential difference of 7 kV exists between them. A length of 20-mm of shrinkable Teflon tubing served as the sample passage between inlet and ionizer.

Performance checks of the inlet-ionizer combination with DIMP in air of 50% RH indicate that the time constant for change in signal was still too long ($\sim 1/2$ hr) for real-time sampling of an air stream. A heating jacket designed for the new inlet holder, which is expected to reduce the response time to about 5 minutes, was not ready in time for testing during the experimental phase of the project. It will be tested in the follow-on phase.

Field Induced Negative Ion Formation

When the polarities of the ionizer potentials and the magnet are reversed, the field ionizer can be operated so as to produce high energy negative ions from electronegative compounds.⁸ The phosphonate structure proved to be ionized and fragmented with relatively high efficiency, producing the negative ions PO_2^- and PO_3^- . These ions are characteristic of organic volatile phosphate or phosphonate products, which can diffuse through the membrane inlet system from an air stream. A negative ion spectrum of DIMP is given in figure 14. The same difficulty with rate of response is present in the negative ion spectrometer as in the positive mode. The sensitivity of detection with a double membrane system is about 40 counts/sec/ppb DIMP in air at equilibrium, and the background is also about 40 counts/sec/amu. The signal-to-noise ratio is therefore equal to the situation in the positive ion mode.



SA-4260-1

Figure 14. Negative Ion Spectrum of DIMP

The sensitivity of detection of the PO_2^- and PO_3^- ions is thus comparable to the sensitivity (signal-to-noise ratio) for positive parent ion detection. The presence of two characteristic ions in equal numbers can lead to a detection device that can look for a simultaneous increase at two mass numbers and therefore significantly improve the signal-to-noise ratio (thus reducing false alarms). Furthermore, the negative ion spectrum, in general, is less cluttered with unwanted masses, even at the ppb level, than the positive ion spectrum.

It is expected that GB will produce POF^- and PO_2F^- ions instead of PO_2^- and PO_3^- , respectively. These products would make the presence of GB distinguishable from that of other phosphoorganic compounds. We plan to verify this point in the follow-on phase, using another fluorophosphate as simulant.

It is also conceivable that PO_2^- and PO_3^- (or correspondingly POF^- and PO_2F^-) will be formed from DIMP (and GB) on electron impact. We may gain detection efficiency this way (mainly because of the nondivergent nature of electron impact-produced ions), but we do not expect improvement in the ratio of signal to chemical background. In fact, it is more likely to deteriorate under electron impact conditions. In any case, in the follow-on phase, we plan to install an electron impact source on the same sector magnet instrument to test these assumptions.

The "inverse" field-induced negative ion formation technique has one potential advantage over field ionization: the problem of source deactivation may be less severe because lower fields may be sufficient for this process, and the negative ion formation does not necessitate the mediation of carbonaceous dendrites.

IV CROSS CALIBRATION EXPERIMENTS

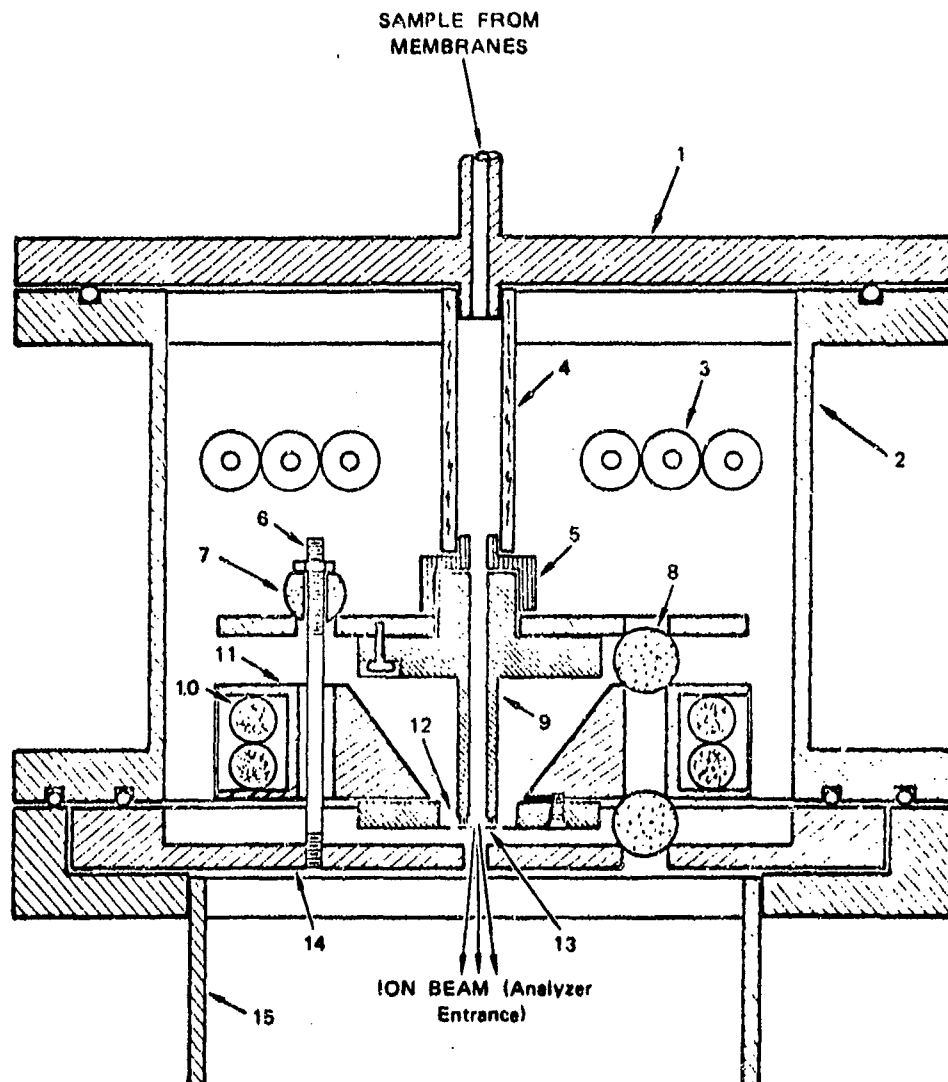
In the first phase of this project, we proved that FIMS is an adequate air monitoring technique for detecting sub-ppb quantities of DIMP. These conclusions were corroborated using more advanced versions of multipoint FI sources. It remained to be tested, however, whether actual agents such as GB follow the same behavior in a FIMS as their simulants, e.g., DIMP. A cross calibrated experiment was conducted to compare the behavior of GB and DIMP.

In the first phase of this experiment, a transportable quadrupole mass spectrometer designed and constructed by Varian Associates was transferred to SRI and modified to a FIMS. Following modification and testing, the instrument was shipped back to Edgewood Arsenal to measure both DIMP and GB under the same conditions. This section describes these tasks and their results.

A. Modification of the Mass Spectrometer

The vacuum chassis of the Varian vapor surveillance quadrupole supplied by Edgewood Arsenal was first disassembled and modified to substitute the SRI multipoint field ionization source (MPFI) for the electron impact source supplied with the instrument. A side view of a typical MPFI assembly with ruby insulators and grid (counterelectrode) heater was shown earlier in figure 7. Kovar is used for the baseplate and heater assembly to match the thermal expansion of the metal parts to the spherical insulators.

Figure 15 shows the details of the adaptation of the MPFI to the ionizer chamber on the Varian mass spectrometer. A new ionizer mounting plate was fabricated to match the fastening pattern on the



- | | |
|---|--|
| 1. Cover Plate (New) | 8. Sapphire Insulator (Not Drilled) |
| 2. Source Chamber | 9. "Spectromat" Multipoint Source Pedestal |
| 3. Electrical Feedthroughs (High Voltage, Heater, Thermocouple, etc.) | 10. Heater Assembly |
| 4. Quartz Sample Feed Tube | 11. Heater/Grid Mount Machining |
| 5. Adaptor Nut | 12. Grid (Counter-electrode) |
| 6. Source Retaining Stud | 13. Multipoint Array |
| 7. Sapphire Insulator (Drilled) | 14. Ionizer Mounting Plate |
| | 15. Quadrupole Chamber |

SA-4250-2

Figure 15. Bottom View of Multipoint Field Ionization Source

counterelectrode/heater assembly. Three sapphire insulators were used to locate the ionization source. Studs pass through the ionizer assembly and drilled sapphire insulators to retain the source. A new cover for the ionizer chamber was fabricated to allow direct sample feed from the membranes to the ionizer. The sample passes through a quartz tube, which is connected to the back of the ionizer pedestal by an adaptor.

The ionizer mounting assembly was also modified. First, the baseplate diameter was reduced. This facilitated electrical connections to the heater by eliminating material that would normally mask the heater from the electrical feedthroughs. Second, the counterelectrode retaining ring was machined away to allow the use of a later version of grid holder assembly. The new grid assembly permitted adjustment of the spacing between the multipoint array and the grid without disassembling the entire ionizer.

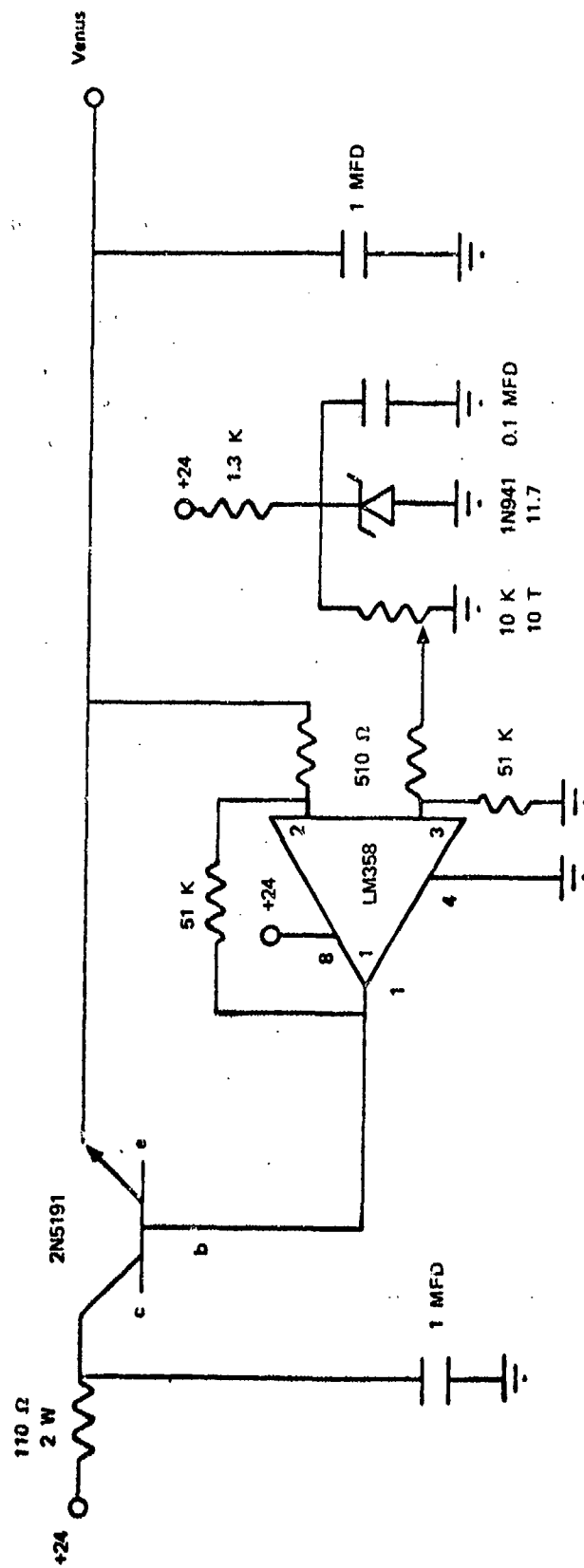
The electrical feedthroughs in the ionizer chamber were tested for breakdown in air. Since they broke down at about 3.2 kV, and the ionizer normally operates at less than 2 kV, they were retained. Electrical connections required by the ionizer include the heater (0-6 V AC), which is floated at the grid voltage; the grid (0 to -3 kV DC); the multipoint array (0 to 24 V DC); and the iron constantan thermocouple, which indicates the temperature at the baseplate of the ionizer. Iron and constantan wires were also used to connect the thermocouple feedthroughs to wires outside the heated analyzer portion of the vacuum chassis to ensure an ambient reference temperature for the source temperature pyrometer.

The high voltage connections to the vacuum chassis for the MPFI were made with high voltage BNC connectors (grid, floated DC heater). Low voltage connections for the thermocouple and multipoint array

(ion energy) were made with a three-pin microphone jack. Part of the sheet metal chassis that surrounds the ionizer chamber was removed to allow clearance for the high voltage leads.

We considered modifying the electronics supplied with the instrument to fulfill the power requirements of the MPFI, but this would have considerably complicated any subsequent reconversion to the electron impact ionization mode of operation. Therefore, we constructed separate electronic chassis for the MPFI. In this manner, we were able to leave all the circuitry for the electron impact source intact and operational. The only modifications made to the electronic chassis of the original instrument were the replacement of the 24-V power supply connector with a 4-pin microphone connector and the addition of 2 wires from the connector to the 115-V leads to the electron impact ionizer's filament power supply. The 115-V power for the filament power supply was interlocked to the vacuum system overpressure relay. We use this connection to activate a relay in the field ionizer chassis to turn off the ionizer high voltage and heater in case of a vacuum accident. It should be noted that the quadrupole electronics (white switch on the original panel) must be turned on to energize the relay and allow operation of the field ionizer or heater. Since the MPFI must be baked before operation, the quadrupole electronics are allowed to come to thermal equilibrium during the breakout period.

The schematics for the field ionizer chassis are shown in figures 16 and 17. Two OEM power supplies were used. A Power Tech 2E24-11 power supply was used to provide the 24-V DC (~ 10 A) that is required by the original electronic chassis for the heaters. A Venus Q-30 photomultiplier supply was used to supply the high voltage for the MPFI (grid voltage). Ion energy (voltage on the "points") was controlled by a 5-k Ω potentiometer that allowed variation of the ion energy from 0 to 24 eV. Originally, the high voltage output of the



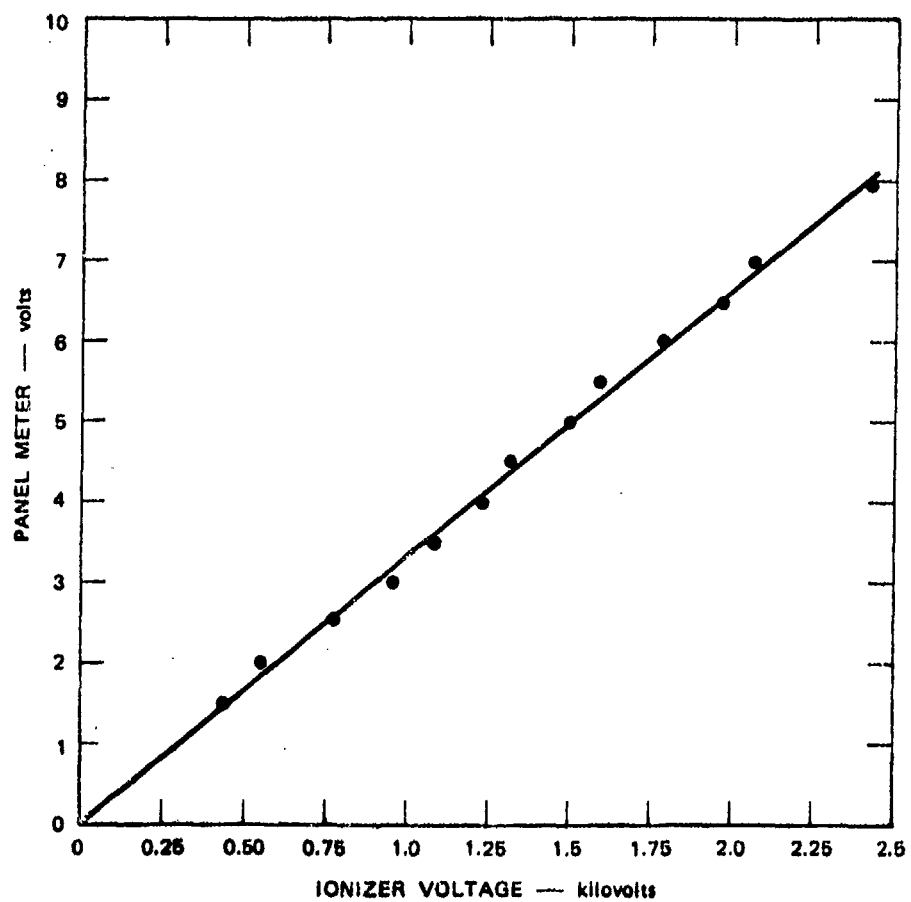
SA-4250-4

Figure 17. Ionizer High Voltage Power Supply Input Regulator Circuit

Venus supply (500-3000 V DC) was controlled by a 2.5-k Ω potentiometer on the voltage input, as shown in Figure 15. We had hoped that ionizer problems caused by overvoltage could be prevented by the power-limiting characteristics of this circuit. (As ionizer current increased, the input voltage would feed back, thereby regulating the ionization potential between the grid and points on the MPFI.) This circuit was not satisfactory, however, so we built the circuit shown in figure 16. This regulator circuit was designed to maintain constant preset voltages on the voltage input, regardless of the current drawn by the power supply. A voltmeter was provided to monitor the ion energy (the input voltage on the power supply). Figure 13 plots the output high voltage to the grid versus the input voltage on the meter.

The source heater was provided with low voltage (-0 to 6 V) alternating current by means of a 6-V filament transformer with a Variac powerstat to control the voltage on the transformer primary windings. A Daytron Model No. D14769 isolation transformer was used to permit floating of the heater at the grid voltage. A pyrometer was provided to allow monitoring of the temperatures of the ionization source. The powerstat was usually set at 40 (indicated) on the panel, which results in a source temperature of about 160°C. Operation of the source at significantly higher temperatures (>200°C) were detrimental to source performance because the tantalum heater wires would begin to evaporate, coating the sapphire insulators with a conducting metallic film that is difficult to remove. Several hours were required for the ionizer to reach thermal equilibrium.

The vacuum system and relay rack were also modified. The organization of the relay rack was altered to include the new electronic chassis, which was placed between the vacuum chassis and the existing electronic chassis. This separated the heaters in the vacuum chassis from the quadrupole electronics, resulting in somewhat improved stability.



SA-4250-5

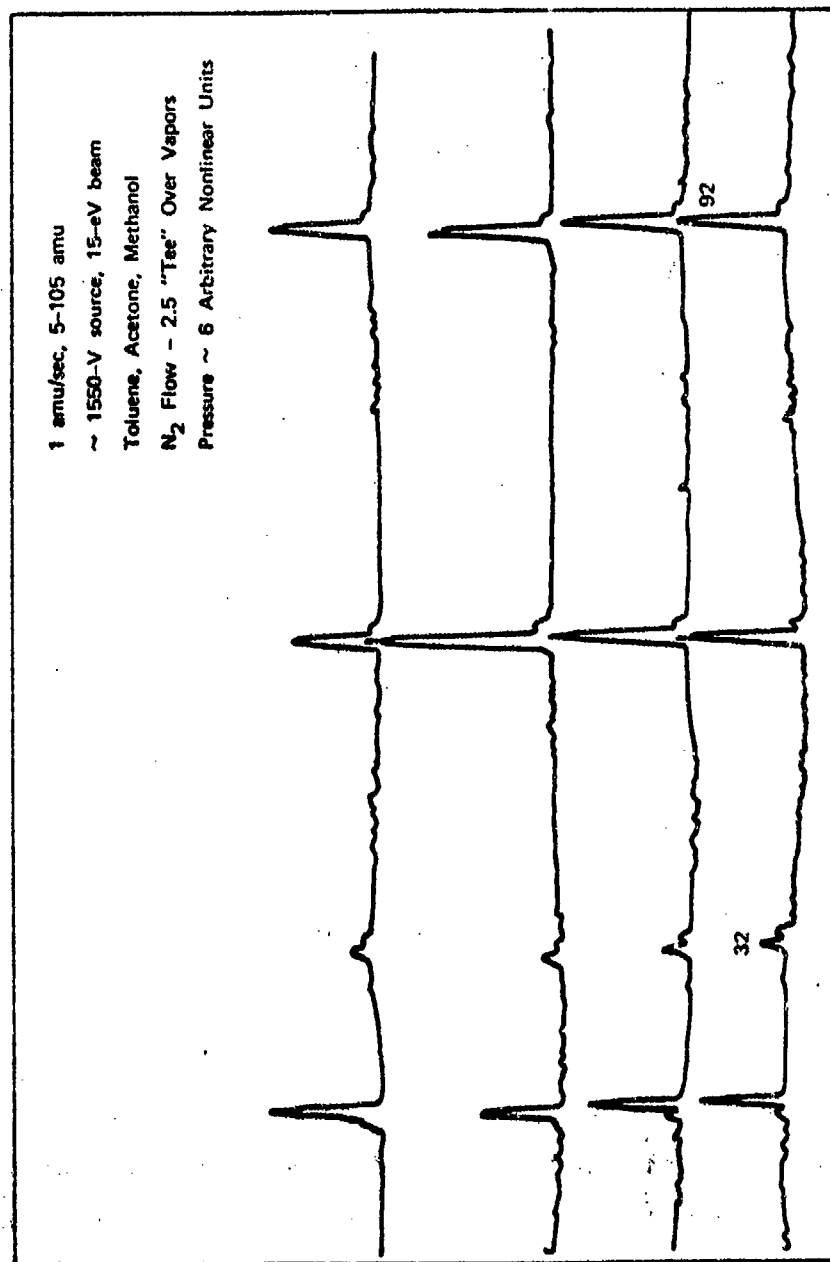
Figure 18. Grid Voltage

During our original evaluation of the instrument, the electronics drifted significantly. Drift in the new configuration versus time is shown in figure 19. The additional space required for the added electronic chassis dictated minor modification to the forepump connections. The foreline was also modified to include a small molecular sieve trap to reduce backstreaming into the canisters used to pump the membranes.

Figure 20 is a plot of the pressure in the Vacion pump, as indicated on a 5-kV Vacion supply, versus the panel meter indication. This calibration was done for several reasons. First, we wished to know the system pressure to evaluate the performance of the MPFI. Second, we experienced some difficulty with the pressure relay in the original electronics; i.e., the relay tripped out before reaching the overpressure zone on the panel meter. This was apparently a spurious effect, which we did not correct, but in operation we reset the trip point on the pressure relay board when problems occurred.

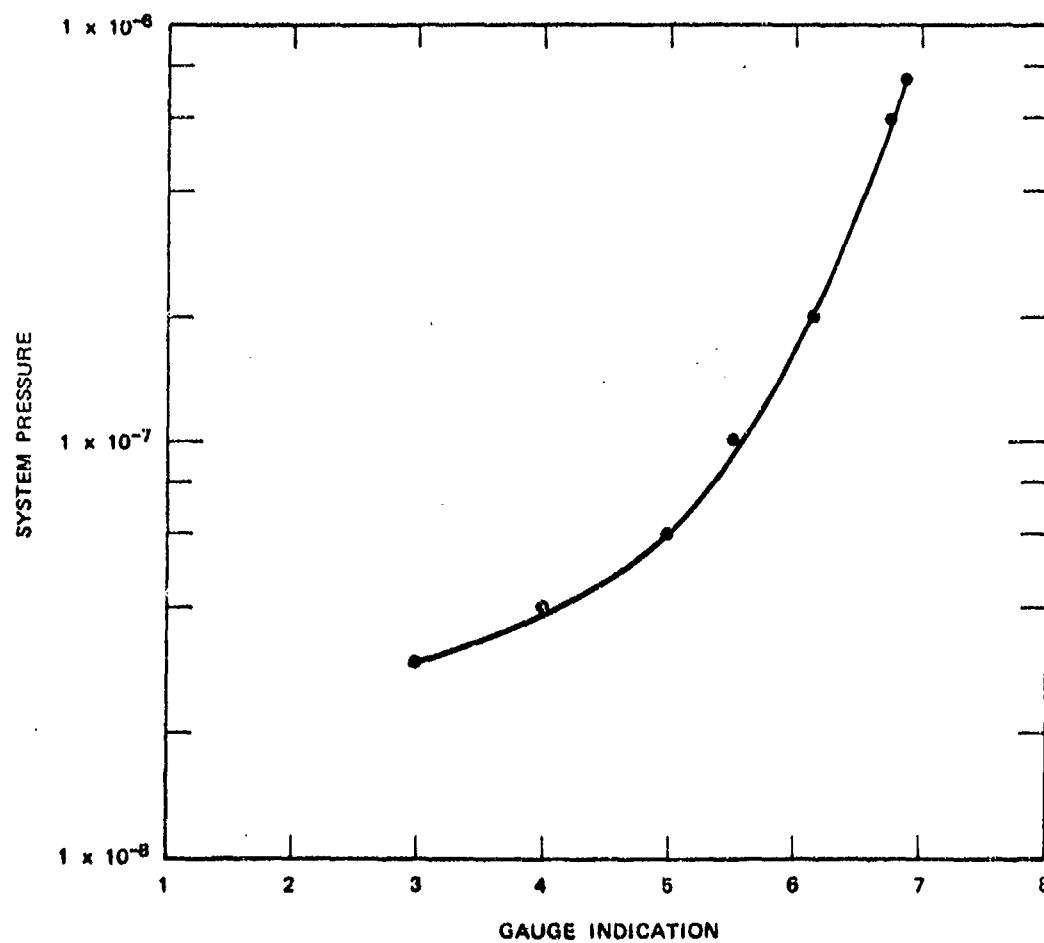
We also experienced a problem with the electrometer board in the original chassis. Inspection showed that part of the circuit was not receiving the supply voltages because of poor contact at the board connectors. Cleaning remedied the problem, but it recurred several times later.

The Varian triple membrane holder was adapted to the 1/4-inch heated inlet lines of the gas phase inlet probe. The holder was fitted with plumbing to provide sample inlet and outlet lines, an intermembrane pumping line with separate flow controlling valves, and the reducer for adapting the 1/2-inch detection inlet to the 1/4-inch inlet probe. The holder was then wrapped with heating tape and insulation to maintain the membranes at 50-60°C. The temperature was monitored with a thermocouple fitted to the holder.



SA-4250-6R

Figure 19. Quadrupole Drift over Time



SA-4250-7

Figure 20. System Pressure versus Gauge Indication, Edgewood Quadrupole

A dilution system for generating an air stream of approximately known simulant concentration was mounted near the inlet system. Laboratory air was filtered through a bed of exhausted Drierite and glass wool before passing through the flow measuring meter and valves. The low level flow of simulant was provided by a cylinder of compressed nitrogen.

Excess sample stream was generated and directed to flow past the sample inlet line of the membrane sampling head. A portion of the sample stream was drawn across the first membrane by vacuum from a small mechanical pump. Flow was controlled with a needle valve and measured with a flow meter. Standard sample flow was set at 2.8 liter/min; at this level increased flow no longer increased the instrument signal level with xylene at 5 ppm in air.

Adjustment of the two intermembrane cavity pressures had little effect on the sensitivity of the instrument to simulant in air, the pressure levels were therefore set in the most convenient manner. The inner cavity was allowed to rise to its equilibrium pressure with the pumpout line shut. The outer cavity was throttled until the mass spectrometer source pressure, as measured by an ion gauge in the sonic region, rose by 5×10^{-7} torr. The inner cavity was then pumped to maintain the increase in source pressure at 1×10^{-7} torr. This then was the operating point in testing the efficiency of sources in cross calibrating the magnetic sector with the quadrupole mass spectrometer.

We constructed a two-membrane holder to compare its enrichment factor and ease of operation with the three-membrane unit. Construction consisted of three stainless steel segments between which the two 1-inch-diameter silicon rubber membranes could be mounted. The membranes were backed with sintered glass for early experiments, and with Monel metal woven screen covered with 100-mesh etched nickel screen in the later experiments.

The assembled holder was mounted with the heated glass gas inlet system and introduced into the mass spectrometer as a unit. The holder was then wrapped with heating tape and insulation to allow the membranes to be held at 50-60°C. The intermembrane cavity was pumped through a flow controlling needle valve by a rotary pump maintaining 10^{-2} torr pressure. The needle valve was adjusted to give a 1×10^{-7} torr pressure rise in the source chamber.

B. Evaluation of the Instrument, DIMP Cross Calibration

In the optimization of the quadrupole mass spectrometers for routine operation with field ionization sources, we have found a number of important factors governing the sensitivity of the instrument. The most significant factor is the proximity of the field ionization source to the entrance of the mass analyzer. The ionizer must be placed as close to the entrance of the quadrupole as possible because the large angular divergence associated with the ion beam emitter from the MPFI causes the brightness of the ion source to fall off very rapidly with increasing distance. The vapor surveillance quadrupole limits the ionizer-to-entrance spacing because the insulators used to retain the analyzer rods protrude into the region where the MPFI would normally be mounted. The brightness problem is further compounded by the need to decelerate the initially divergent beam emitted from the MPFI from > 1 keV energy to ~ 20 eV. Since this deceleration diverges the beam still further, it is doubly important that the ions experience the focusing effects of the quadrupole RF field as quickly as possible, i.e., that the source exit be as close as possible to the RF field. This will be discussed more in detail in Section V B.

Another factor affecting transmission in the quadrupole, and therefore instrumental sensitivity, is the diameter of the quadrupole rods. The transmission of quadrupoles decreases at any given resolution

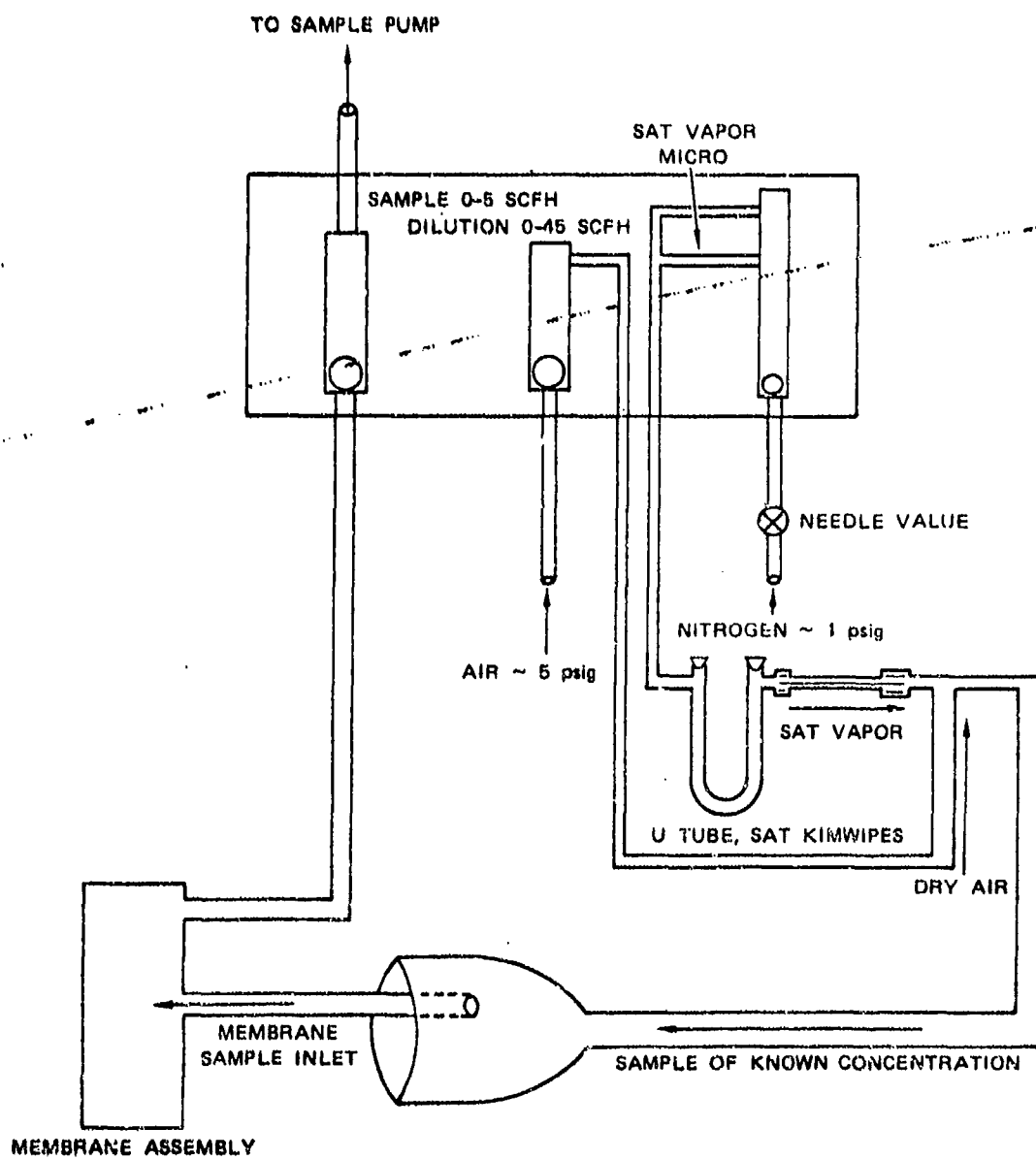
with smaller analyser rods. The rod diameter in the vapor surveillance quadrupole appears to be approximately 6 mm, which is considerably smaller than the 15.3-mm-diameter rods we normally use. Mechanical alignment of the rods also affects ion transmission, but we could not check this on the vapor surveillance quadrupole, since we do not have the proper equipment.

We have also found an improvement in transmission when care is taken to properly terminate the exit and entrance RF fringe fields. The extranuclear quadrupoles we normally use are equipped with the "ELF option," a ferrite insert that gradually terminates the RF fields of the analyzer at the entrance. The vapor surveillance instrument has no comparable provision.

Finally, we normally use continuous dynode electron multipliers in the counting mode. Continuous dynodes provide a much better signal-to-noise ratio than the discrete dynode type $2s\ 2n$ analog device used in the vapor surveillance quadrupole.

The field ionization conversion was initially evaluated with acetone, toluene, and methanol because these substances are known to activate the MPFI. Typical spectra obtained from a mixture of the three compounds were shown earlier in figure 19. The sample was introduced into the triple Llewellyn membrane inlet system by flowing a small quantity of nitrogen over a tube containing a mixture of the three solvents. No attempt was made to measure the concentrations introduced because the objective at that point was to become familiar with the instrument in its modified form and the activation of the MPFI.

The first quantitative sensitivity measurements were made with the sample flow system shown in figure 21. A measured flow of nitrogen was passed over laboratory tissues saturated with the compounds of



SA-4250-8

Figure 21. Sample Inlet Flow System

interest in a U-tube. The known flow of vapor that exited the U-tube could then be diluted with a measured flow of air. The diluted sample was then fed to a glass chamber, which surrounded the membrane sample inlet and vented to atmospheric pressure. A pump was used to draw the sample out of this chamber and over the membranes. The sample concentration was calculated by assuming that the vapor leaving the U-tube was fully saturated at room temperature and pressure. Volume flow rate across the membranes was about 2 liter/atm/min.

The first sensitivity measurement was made with xylene (106 amu) with the quadrupole tuned for a constant Δm of 0.5 amu measured at one-half the peak height. The concentration of xylene required for an adequate signal-to-noise ratio (~ 4 to 1 on the 10^{-8} range of the electrometer) was about 1 part in 25,000. The MPFI was operated at 1700 V and 15 eV ion energy, and the analyzer pressure was about 1.8×10^{-7} torr. The spectrum obtained with xylene is shown in Figure 22.

We then measured the sensitivity of the instrument with bis(2-chloroethyl) ether, as shown in Figure 23. The resolution of the instrument was reduced to a minimum to ascertain the threshold sensitivity obtainable with the compound. At 1 part in 250,000, the signal-to-noise ratio was about 2 to 1, and there was virtually no valley observable between peaks 2 amu apart. The ionizing voltage was 2000 V and the ion energy was 24 eV.

DIMP was then run at the same resolution. With a source voltage of 2100 V and signal-to-noise ratio of approximately 1 to 1, one part in 760,000 could be seen by repetitively scanning and noting that DIMP appeared in the same location in each scan, as shown in Figure 24. The system pressure was 3×10^{-7} torr, which was maintained by throttling the pumping on the membrane cavities. With an external electrometer connected to the multiplier output, the maximum current reading obtained for DIMP was $\sim 1 \times 10^{-11}$ A. If we assume a gain of $\sim 10^4$ for the electron multiplier, the transmitted and detected ion current was $\sim 1 \times 10^{-15}$ A.

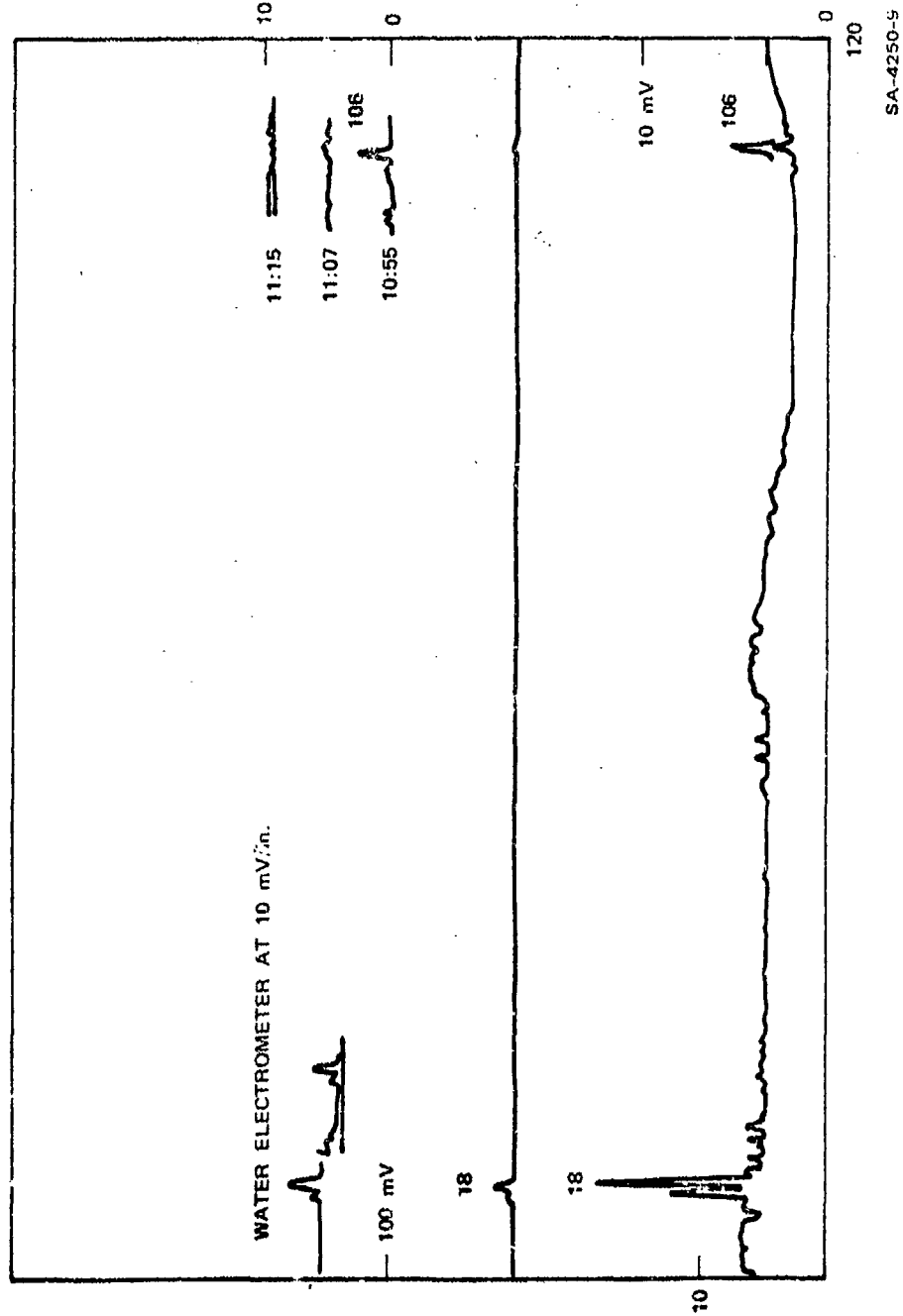
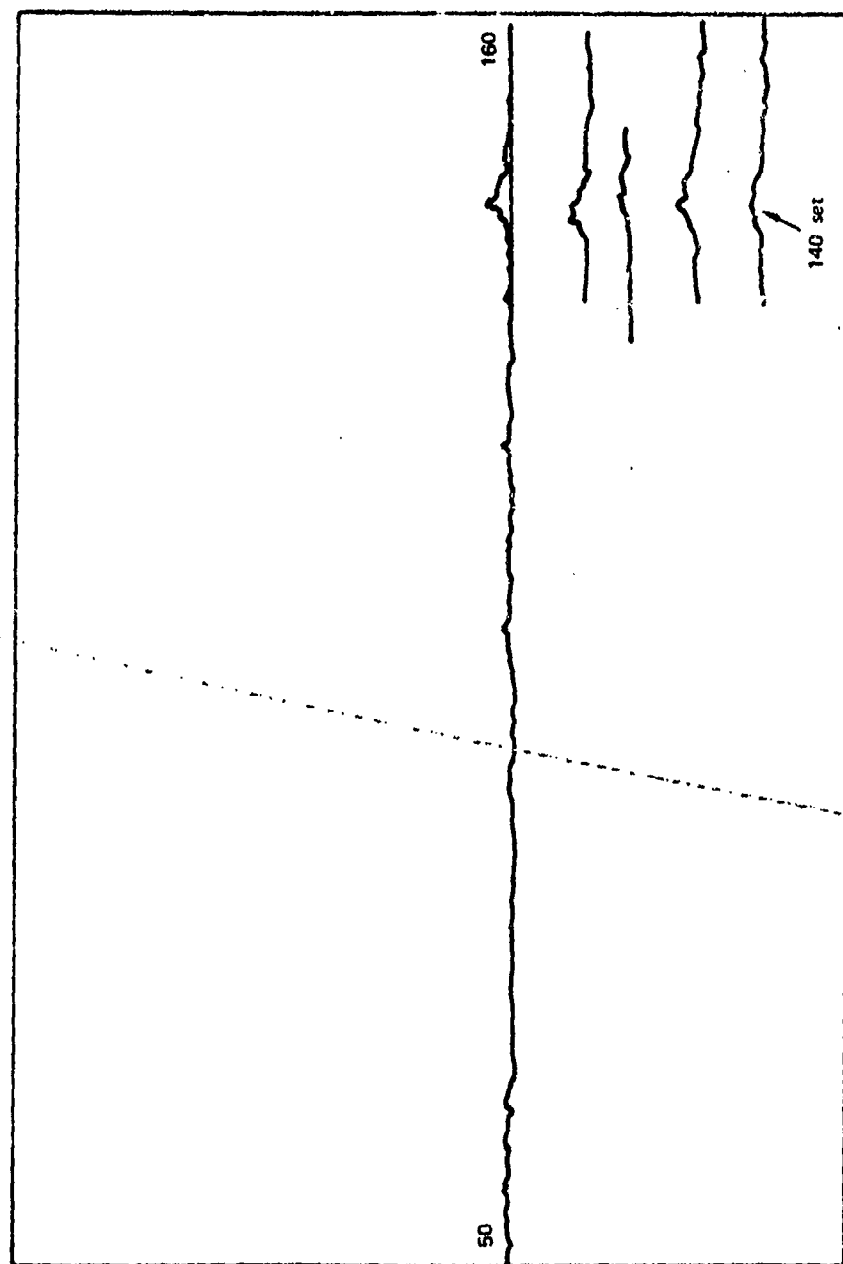
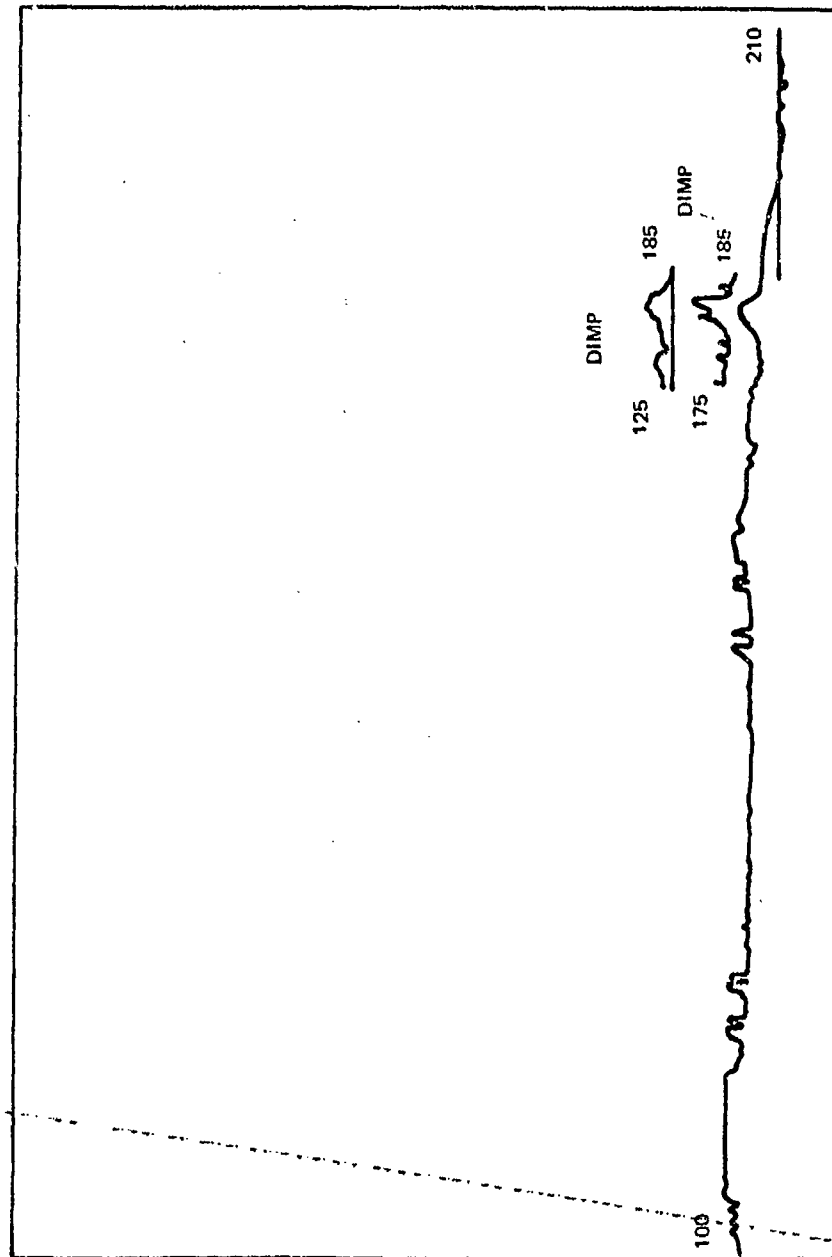


Figure 22. Sensitivity Measurement with Xylene



SA-4250-10

Figure 23. Sensitivity Measurement with Bis(2-chloroethyl) Ether



SA-4250-11

Figure 24. Sensitivity Measurement with DIMP

The instrument was examined to see whether careful tuning could be used to improve its sensitivity. The DC circuit was carefully adjusted using the procedures described in the Varian manual. The resolution and offset controls on the front panel did not function in the desired manner with the instrument adjusted. Some iteration was required on the inverting amplifier to obtain adequate control over resolution. The quadrupole functioned best with some offset in the DC supplied to the rods. The ratio of AC voltage to DC voltage was adjusted empirically as suggested in the instruction manual. The RF circuit was tested and found to be functioning satisfactorily.

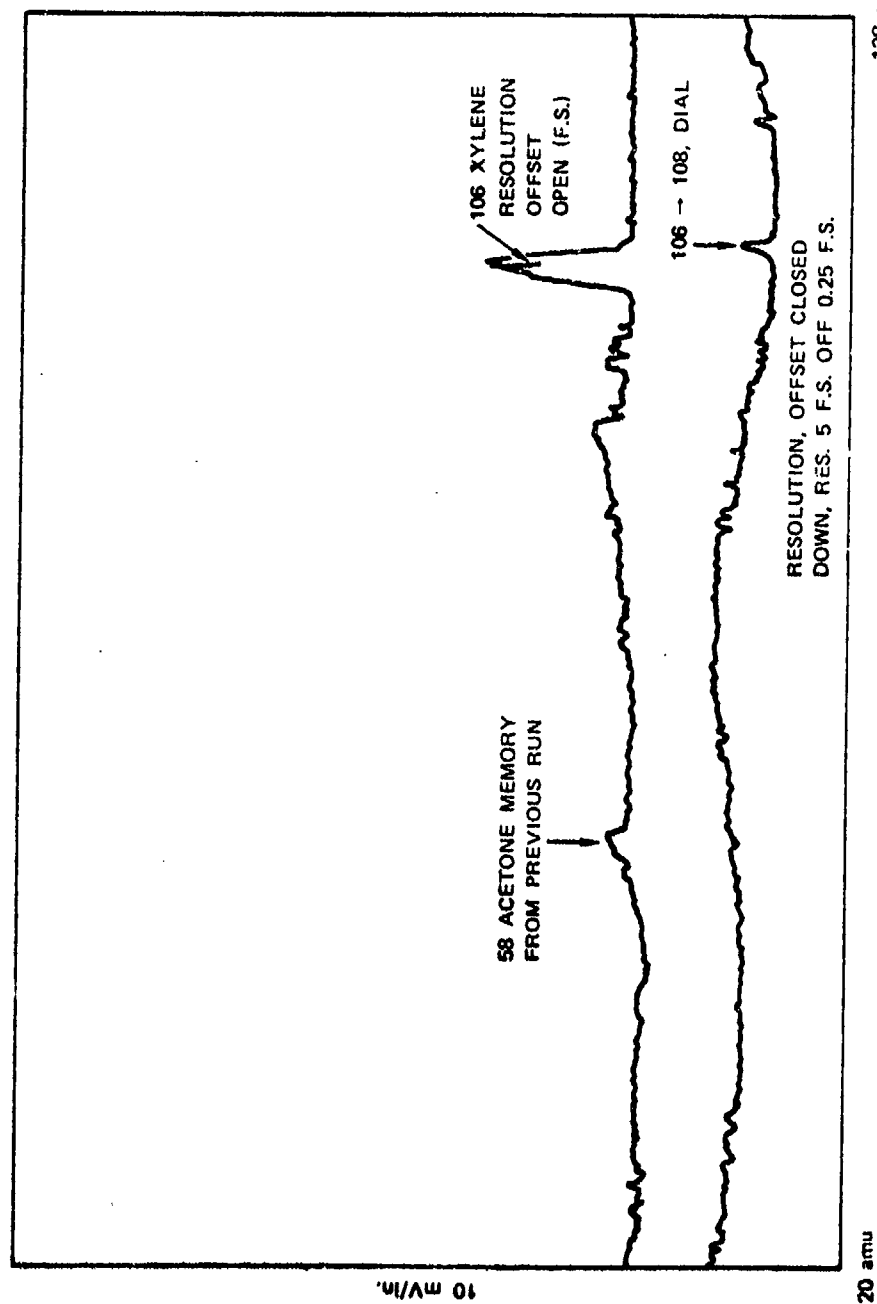
Since there was nothing obviously wrong with the quadrupole electronics, we removed the MPFI to see whether it had been damaged. Several of the points had melted back, which is normal, but nevertheless a second set of points was installed. Since no significant changes were noted in the performance of the instrument with the new source, it was concluded that the total instrument was functioning normally, but that the instrument was marginally sensitive for giving a reliable cross calibration.

The sensitivity of the Extranuclear quadrupole was $1/6$ that of the magnetic sector with DIMP simulant at $1/3$ the resolution (~ 100 quadrupole vs. ~ 300 magnetic sector). We found that the field ionization source, as optimized for multicomponent analysis of oil samples, was more sensitive to deactivation than the source used in the magnetic sector. The quadrupole source is used at a closer spacing and lower field to lessen the energy spread and the analyzer dispersion of the generated ions. The sensitivity of the quadrupole decreased steadily during the run, reaching the reported sensitivity at its equilibrium level. - The same phenomenon occurs with a highly conditioned source on the magnetic sector instrument, but the loss in sensitivity can be offset by increasing the ionizing field strength.

The Extranuclear quadrupole was thus just 6 times less sensitive than the magnetic sector instrument and therefore about 200 times more sensitive than the modified Varian instrument. These findings were reported to the Contact Project Officer, who determined that additional extensive modification of the vapor surveillance system was not cost effective and that in spite of its shortcomings, the quadrupole system should be returned to Edgewood Arsenal, as already modified, to attempt a cross calibration test.

Before the instrument was shipped, it was restarted to check the reproducibility of our earlier sensitivity measurements. Xylene was used to activate the ionization source and to check the instrument's operation. After each xylene run, a measured concentration of DIMP was fed to the membranes. From the first xylene run, we found that retuning the instrument from a peak width of 2.5 amu at half the peak height to a peak width of 1 amu reduced the sensitivity by a factor of 4 at mass 106. With a xylene concentration of 200 ppm, the electrometer output was 10 mV on the 5×10^{-8} range at the lower resolution. Signal-to-noise ratio was about 5 to 1. The spectra obtained with xylene are shown in figure 25.

DIMP then introduced at a concentration of 0.8 ppm produced no detectable signal. The DIMP concentration was increased to 1 ppm following another xylene run, but the signal was still too low. During this run, the concentration was gradually increased until the DIMP signal could be positively identified. The signal-to-noise ratio was so poor that several scans were required for verification. The sample concentration could not be accurately determined because the system had not reached equilibrium. In an effort to obtain more signal during this run, we also used significantly higher ionizing potentials than normal for quadrupole operation (2200 V instead of the <1800 V required for xylene). This is normally not desirable since the



128 amu
SA-4250-12

Figure 25. Sensitivity Measurement with Xylene before Shipment of Instrument

probability of damaging the ionizer is increased at higher grid-to-point potentials, with the close spacings normally used for quadrupoles, and also, the background noise level increases under these conditions.

The best DIMP results that we were able to obtain are shown in figure 26. The sample concentration was 7.7 ppm. The machine was operated for about 6 hours at this concentration with the MPFI "idling" at 1700 V. The electrometer was on the 10^{-9} scale. During the scan period shown, the ionizer voltage was increased to 2250 V.

We observed during this set of experiments that the water peak disappears during the DIMP runs, indicating that the sample deactivates the source. Further evidence of deactivation was found when xylene was introduced after a DIMP run. The source required 15 to 40 minutes of activation with xylene to reach the baseline value established for xylene before the introduction of DIMP. This deactivation of the MPFI by DIMP may be a significant factor in the generally poor performance observed from the instrument. We concluded that the initial low sensitivity of the quadrupole requires such high concentrations of DIMP to observe any ion current that the source was being deactivated in a very short time. This further reduced the overall system efficiency, making it difficult to reproduce measurement. If the analyzer efficiency were higher, the minimum detectable concentration of DIMP would be lower and the source activation would be longer lived. Therefore, this downward spiral of sensitivity would not occur in other instruments.

Two experiments were attempted in an effort to overcome the deactivation problem. First, xylene was mixed with the DIMP in the U-tube. Deactivation still proceeded very rapidly even though xylene normally activates the MPFI.

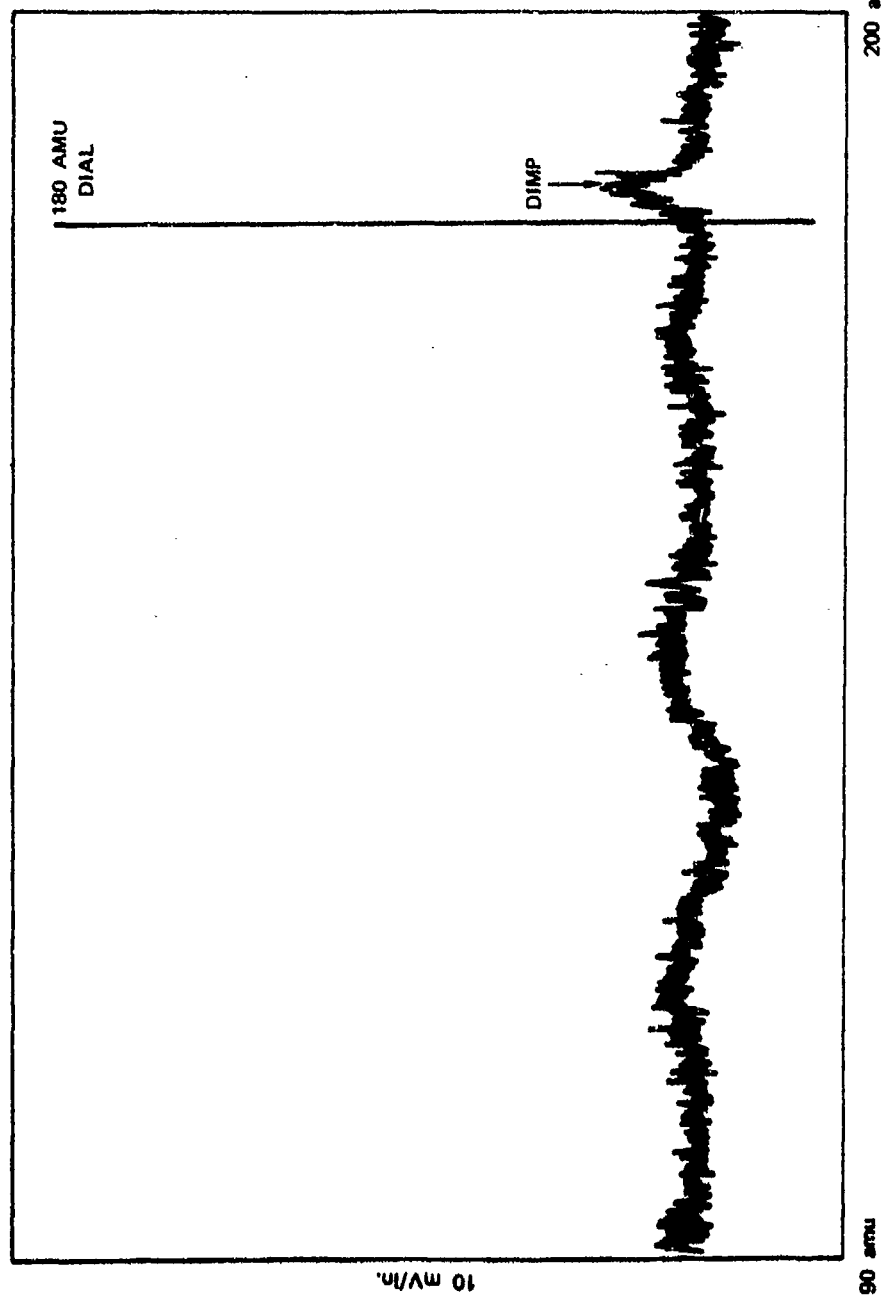


Figure 26. Sensitivity Measurement with DIMP under Continuous Input

In the second experiments, the system was allowed to reach sample flow equilibrium with the MPFI activated, but turned off to avoid deactivation. Then the ionizer was suddenly turned on and the DIMP signal measured. The signal level obtained by this procedure was not significantly greater than the levels observed when the source is run at moderate voltage while the sample feed system reaches equilibrium. In normal practice, it is much better to keep some voltage on the source while sampling because the source remains cleaner in this mode of operation. Suddenly applying high voltage to the MPFI, which has collected large amounts of sample, can result in a glow discharge and cause permanent damage to the ionizer.

In conclusion, it was possible to repeatedly observe DIMP at the concentrations noted, but these results could be considered only semiquantitative.

C. Comparison of the Vapor Surveillance Quadrupole's Sensitivity to GB and DIMP

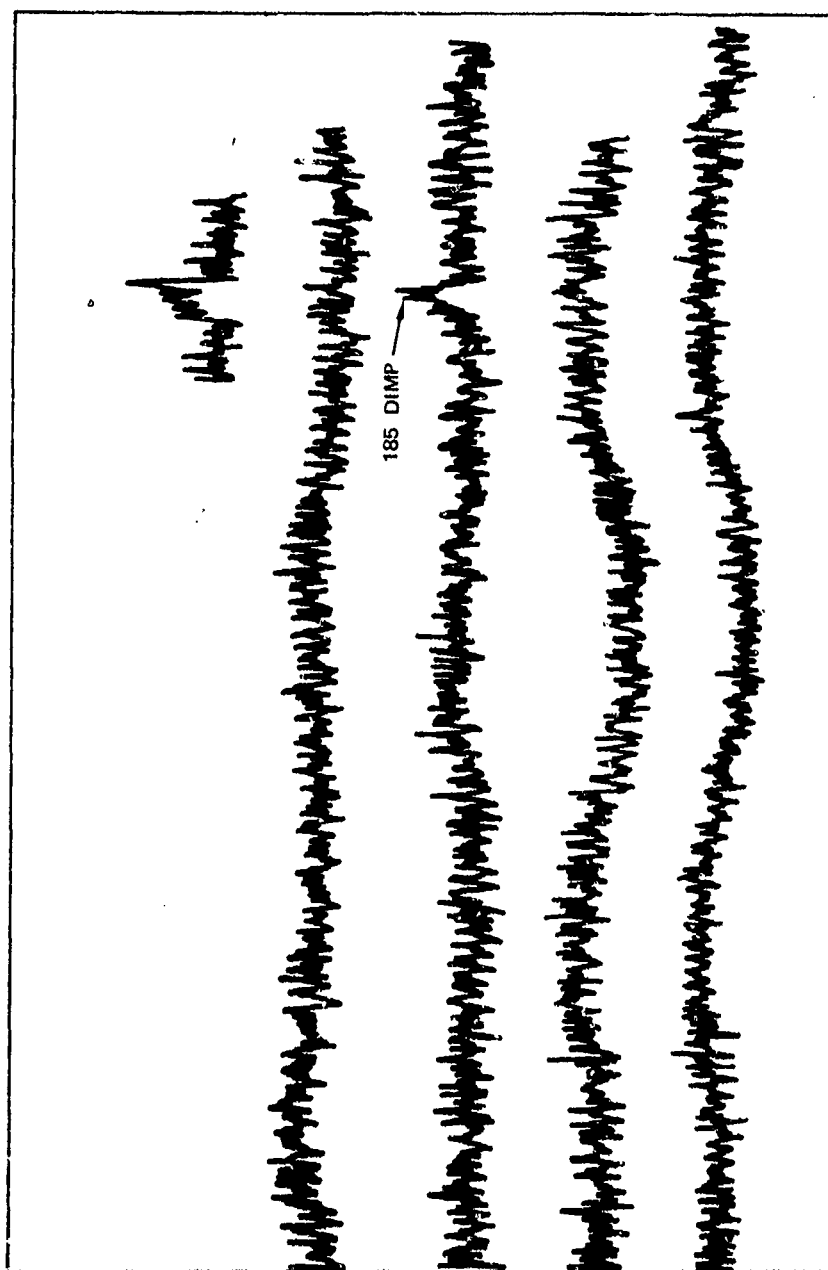
The final series of experiments performed with the combined Varian vapor surveillance quadrupole and SRI multipoint field ionizer was comparison of the system's sensitivity to GB and DIMP. These data were needed because all the previous experiments performed at SRI used DIMP as a simulant for GB.

Robert Cross of SRI went to Edgewood to assist in the performance of the DIMP/GB comparison experiment and to assure that the instrument was performing properly. The instrument was checked out using the sample introduction system normally used at SRI. Xylene was sampled to assure that the multipoint field ionizer was activated. The "generator" system used by Edgewood to provide known concentrations of various agents was then adapted to the Lewellyn membrane inlet system on the mass spectrometer. DIMP was introduced at a concentration of 10 ppm.

The results of this test are shown in figure 27. Comparison of these spectra with those in figure 26 shows that the DIMP determination could be repeated with the instrument at Edgewood using the "generator" system. The earlier spectrum obtained at 7.7 and the electrometer/chart recorder settings were the same for both spectra.

Since the instrument could readily reproduce the DIMP determinations made at SRI, the ionizer was reactivated with xylene to its normal efficiency and a 10 ppm concentration of GB was introduced. Figure 28 shows the spectra that resulted. The lower scan was obtained the instant the GB was turned on. Five minutes later the GB peak had appeared (middle scan). Ten minutes after the initial introduction of the sample, the peak had disappeared even though we increased the ionizing potential from 1750 V to 2100 V. Subsequent GB determinations gave similar results. The peak rapidly appeared upon introduction of the sample and then deteriorated as the ionizer was deactivated. By carefully timing increase of the ionizer potential with the pressure increase in the mass spectrometer produced by the GB entering the system, we were able to obtain slightly larger peaks from the GB than we obtained from DIMP. The differences were not large enough, however, to conclude that the sensitivity of the instrument to GB was significantly greater than its sensitivity to DIMP.

The time required to detect GB with the quadrupole at the 10 ppm level was significantly shorter than the detection time for DIMP. This difference can be attributed to the difference in adsorbability between the two compounds. This information is important since one of the major problems with the DIMP measurements performed at SRI is the long time lag between sample introduction and detection.



SA-4250-14

Figure 27. Sensitivity Measurement with DIMP at Edgewood Arsenal

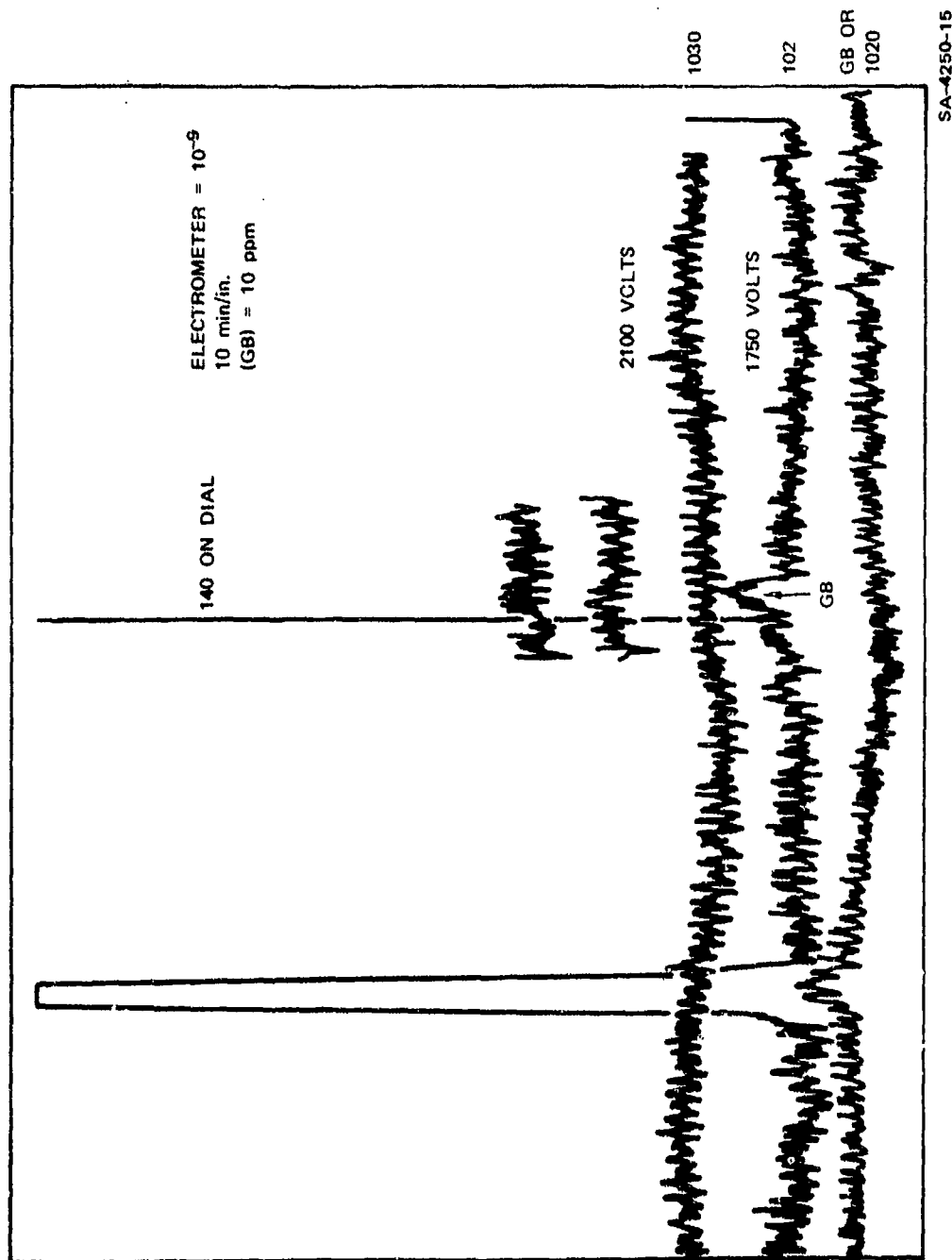


Figure 28. Sensitivity Measurement of GB at Edgewood Arsenal

Several conclusions may be drawn from the results of the DIMP/GB comparison. First, the use of DIMP as simulant appears to be justified and thus the projections on the detectability of GB by FIMS, based on DIMP data, are valid. Second, the deactivation of the multipoint field ionizer by high concentrations of both substances is a primary problem. For reliable detection, an ionizer/mass spectrometer combination must be developed that is sensitive enough to perform low level determinations with a deactivated multipoint field ionizer, or a field ionizer must be developed that is less sensitive to deactivation. The shorter response time noted for GB is encouraging from the standpoint of the operation of the field instrument.

V STUDIES ON FIELD IONIZATION SOURCES

This section describes studies of the efficiency of field ionization sources, the divergence of the exiting ions, the impact of this feature on interfacing the FI sources with quadrupole mass analyses, as well as the start of development of a novel type of FI source. Some of the results described here were cosponsored by NIH grant No. RO1-CA 13312-04.

A. Comparison of the Field Ionization Efficiencies of the Tungsten Activated Wire Field Ionization Source With Multipoint Array Sources

Although activated thin wires are currently the most widely used field ionization emitters, little is known about their efficiency compared with the SRI multipoint sources. Consequently, it was desirable to devise an experiment that would compare the efficiencies of the two sources in a mass spectrometer under similar operating conditions.

The two sources differ in both construction and usual operating conditions. The multipoint emitter consists of an array of tiny pyramids deposited on a screen of 25 μm centers and are about 40 μm high. The purpose of the pyramids or "points" is to enhance the electric field near the tip of the points when the array is placed close to a counterelectrode and a potential applied between the electrodes. The multipoint source is normally operated at 2 kV between the emitters (points) and the counterelectrode with a spacing of 50 μ between them. By lowering this spacing to less than 25 μ , we have been operating these sources at less than 1 kV. Field enhancement for the

thin wire is accomplished by growing microneedles (activation), which are also about 40 μm high on the surface of a tiny tungsten wire. The thin wire is usually operated at 10 kV with 1- to 2-mm spacing.

The sample to be ionized is fed to the points in a multipoint source directly through the screen carrying the points, whereas the thin wire is normally fed by bleeding it into the chamber which constitutes the source assembly. The geometry of the emitting area also differs since the wire is a line source and the multipoint array is circular.

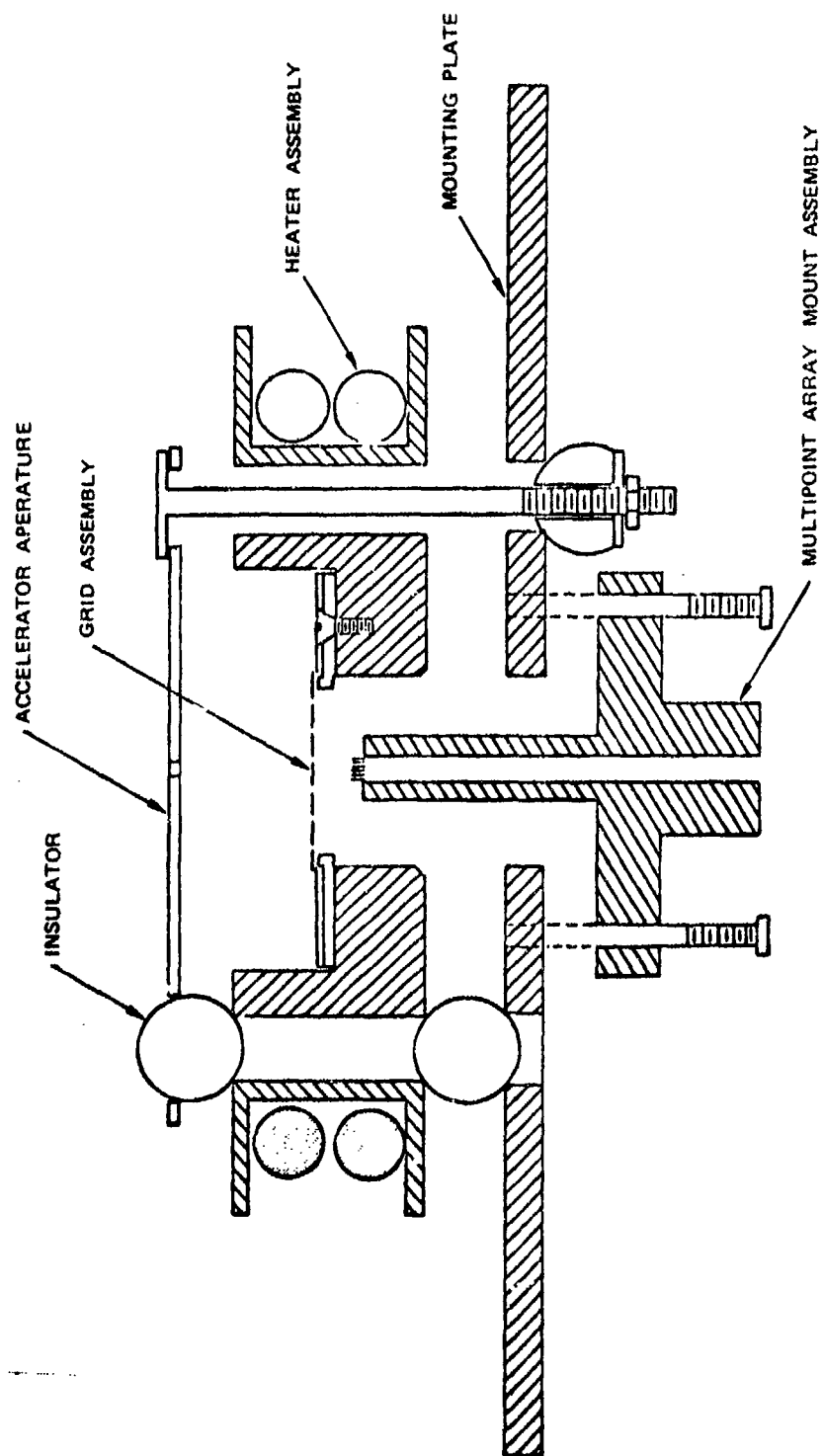
The multipoint sources are much more sensitive to abuse, i.e., excessive pressure buildup between points and grid at a given voltage or excessive voltage at a given pressure. Under these conditions a discharge occurs between the points and grid, melting down the tiny cones and rendering the source useless. Occasionally, a partially damaged source may be reactivated to perform as a useable ionizer but never at the original high ionization efficiency. This pressure buildup or excessive ionization current may occur by resorption or field desorption of trace impurities from the active regions of the source. It is necessary therefore to bake out the source before use and then to raise the voltage very slowly to field-desorb these impurities. Once the source is clean, it may be used for hundreds of hours without deterioration. However, whenever the source is brought up to atmospheric pressure (even without any voltage), the clean-up procedure must be carefully repeated. The thin wire sources are reported not to require this careful pretreatment.

For this series of experiments, the thin wire was adapted to the operating conditions of the multipoint source so that the relative efficiencies could be examined in the same ion source test spectrometer. Obviously, this is a deviation from standard practices for the wire sources; however, it was our desire to standardize the operating

conditions of both sources to make the comparison as fair as possible. The activated wire emitter was operated at 50 μ spacing at voltages similar to those used for multipoint sources. Grids were used as counterelectrodes for both sources to eliminate the centering problems common to slit style counterelectrodes with the thin wire emitters. (We have tried to use a slit counterelectrode for the wire source but, due to alignment problems that required the use of mechanical manipulation, efficiency could not be optimized.)

The sample was fed to the thin wire through a small tube directed toward the center of the activation. Both sources were installed in the same mount assembly, as shown in figures 29 and 30. The result was preservation of the instrument's optical configuration and thus the efficiency for both sources. The problem of different beam geometry (i.e., slit image versus circular image) was solved by stopping down the electron multiplier to measure current density per unit area rather than total ions produced. This has the advantage of allowing direct comparison of efficiencies when viewed as the efficiency per unit area of the emitter.

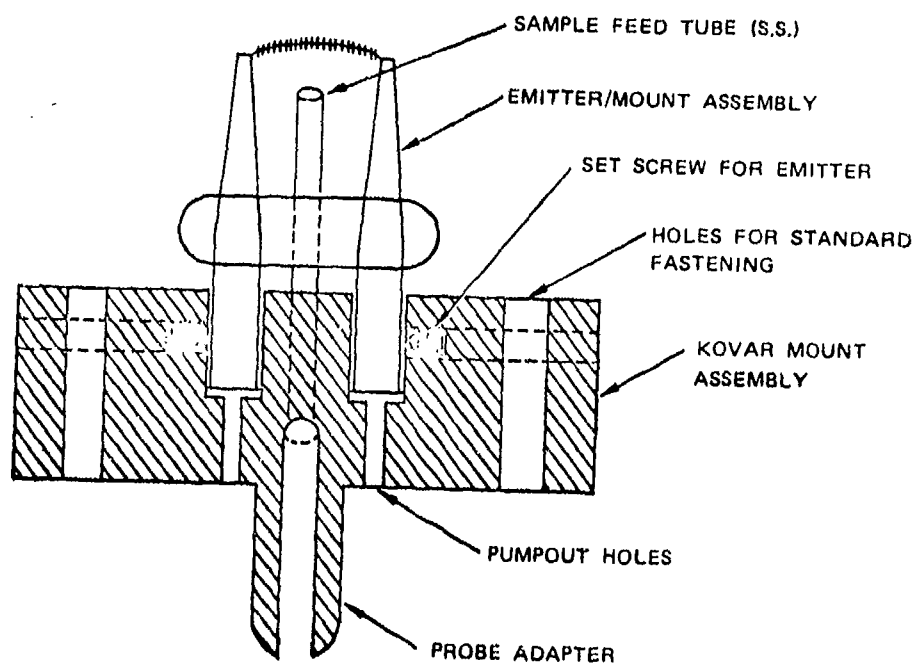
The test instrument (figure 31) uses a Colutron model 300 low resolution ion velocity filter for mass analysis. The ion beam is accelerated to 5 kV by a grounded extracting aperture mounted on the ion source. The beam is focused by two einzel lenses between the source and mass analyzer. Minor geometrical adjustments are made with horizontal deflectors to assure beam centering on the electron multiplier. Mass range could be varied by vertical deflection of the beam. Counting equipment was used to integrate the collected ions for a preset time while maintaining constant sample flow rates.



APPROXIMATE SCALE 4X

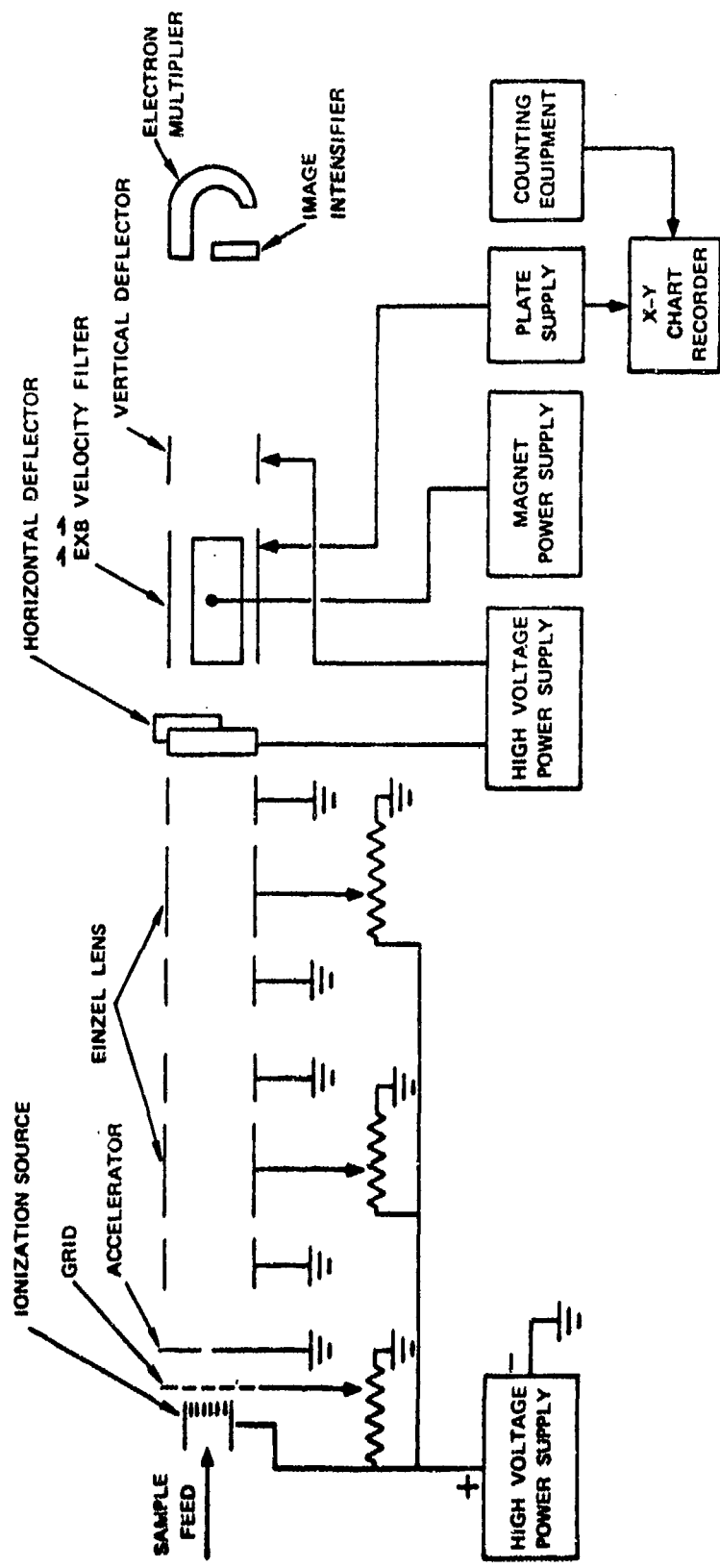
SA-1977-100

Figure 29. Test Arrangement for Multipoint Sources



SA-1977-101

Figure 30. Test Arrangement for Activated Wire Source



SA-1977-102

Figure 31. Schematic of Test Mass Spectrometer

The sample feed system shown in figure 32, consists of an MKS Baratron pressure gauge with a Servo-driven variable leak automatic pressure controller to regulate the ballast volume pressure and thus the feed rate. Pressures in the micron range were maintained automatically with an accuracy of better than 0.1μ . The sample feed system was connected to the ion source by a probe (containing a $50\text{-}\mu\text{m}$ -diameter fixed leak), which was inserted through a vacuum lock.

Flow rate was calibrated by plotting pumpout rate through the fixed leak. Flows in ml/sec (F) were calculated by the relation $F = (V/\Delta t) \ln |P_0/P|$, where V is the volume of the feed system in ml, and Δt is the elapsed time between the pressures P_0 and P. Molecular flow is assumed in this system and wall effects are neglected. Flow in the lines to the fixed leak is transitional, but flow velocity was low so that the possibility of a pressure difference between the ballast chamber and the location of the fixed leak could be neglected. In the leak itself the flow was purely molecular at the pressures used. Since the tests were carried out on a pure substance (1-butene), no fractionation effects in the inlet systems needed to be considered.

As a check, the theoretical conductance of the fixed leak for molecular flow was calculated and compared with the measured values. For the multipoint source, the measured values were lower by a factor of approximately 3.1. The thin wire conductance was down by a factor of approximately 2.0. The difference between calculated and measured values is largely explained by the fact that the molecular leak is not an ideal orifice, the conductance of the probe and ion source are neglected (which could possibly introduce a numerical factor in losses), and finally, the pumpdown of the system through the leak indicated that there are some wall effects in the feed system. To avoid any ambiguity, the values obtained by the empirical calibration were used for the ionization efficiency comparison.

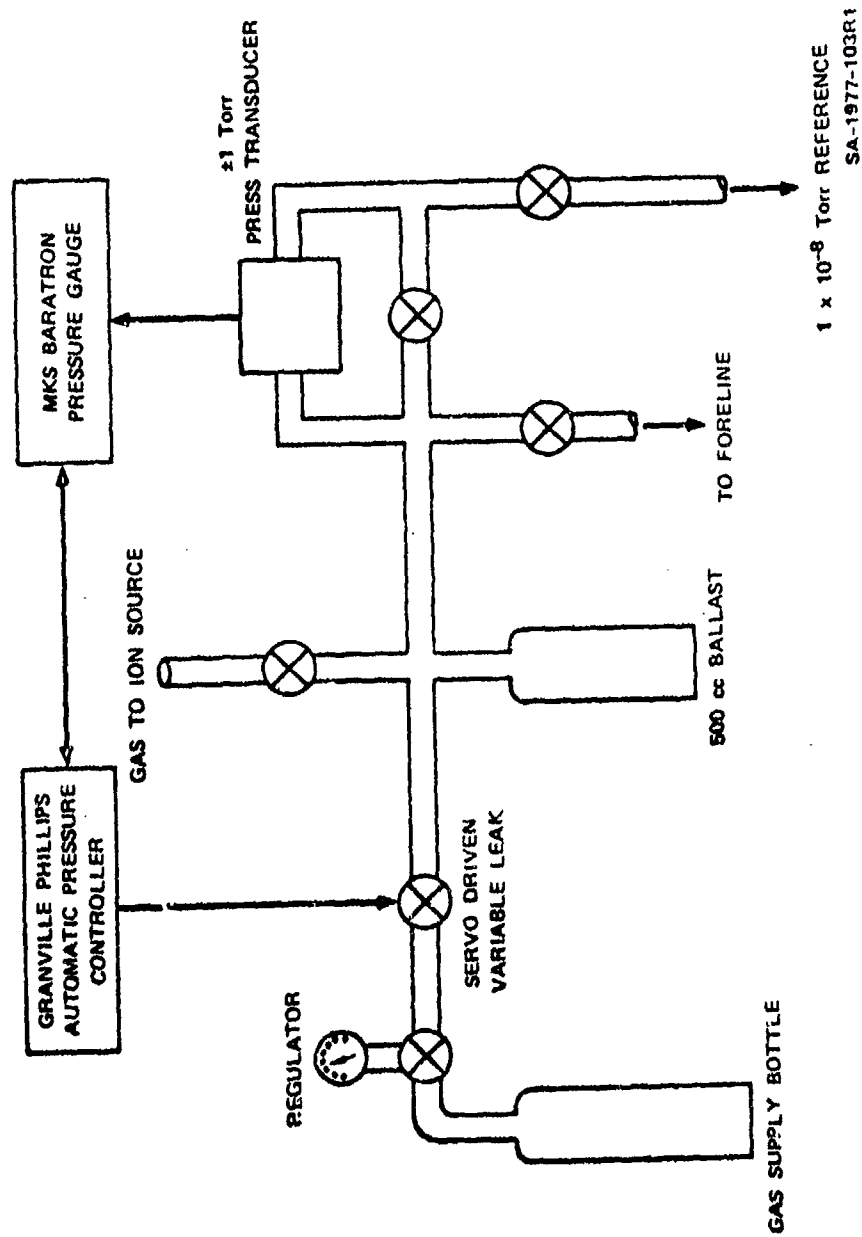


Figure 32. Schematic of Sample Feed System

Measurements were made by fixing sample flow at a constant value and integrating counts for 10 minutes. The procedure was carried out for several different source voltages over a feed system pressure range of 0.01 to 0.03 torr for the multipoint source and 0.1 to 0.3 torr for the thin wire source assembly. The lower pressure used in the multipoint sources, to avoid excessive pressure buildup between points and grid that could lead to discharge, would decrease the relative ionization efficiency of these sources compared with the wire source if the adsorption of the substrate to the field ionizing region were a critical factor and if the operation conditions were below adsorption saturation pressures. The measured flow rates for the multipoint source were 2.66×10^{-11} molecules/sec at 0.010 torr and 7.98×10^{-11} molecules/sec at 0.03 torr; for the thin wire the measured flow rates were 4.13×10^{-10} molecules/sec at 0.12 torr and 1.24×10^{-9} molecules/sec at 0.30 torr. Efficiency was determined by converting total counts to average cps then taking the ratio of $\frac{\text{cps}}{\text{molecules/sec}}$.

The test mass spectrometer used for these measurements does not have a high transmission so that the total efficiency of the ionizer-spectrometer system is lower by about three orders of magnitude than those of our sector magnet instruments. No attempt was made to deconvolute the ionizer efficiency since the same spectrometer was used for all measurements and relative data were desired. The results are tabulated in table 3. Also included in table 3 for comparison are values for an unactivated 250- μm -diameter multipoint source. These are included to indicate the worst efficiency likely to be observed from a multipoint source. The source used for primary comparison was a 1-mm-diameter source, which was removed from one of our spectrometers. The effect of several hours of activation with thymine on the 250- μm array is also shown. In all cases the multiplier acceptance area was a slit 1.78 mm by 0.51 mm, which was smaller than the beam images at that point.

Table 3. Relative Efficiencies of Multipoint FI Sources and Activated Wire Emitters

Source	Emitter to counter electrode potential (V)	Sample feed rate (molecules/sec)	Number of integrations	Average efficiency ^a (ions/molecule)
Activated thin wire	2310 - 2695	3.7×10^{14} to 6.2×10^{14}	13	2.9×10^{-13}
Partially activated multipoint	1540 - 1925	5.3×10^{13} to 8.8×10^{13}	16	8.3×10^{-12}
Unactivated 0.25 mm multipoint	1540 - 2310	5.3×10^{13} to 8.8×10^{13}	20	1.2×10^{-12}
Well activated 1.0 mm multipoint (removed from operating spectrometer)	1925	4.4×10^{13} to 7.5×10^{13}	9	3.5×10^{-11}

^aThese data are relative efficiencies from mass spectrometric measurements uncorrected for transmission efficiency.

The tabulated values show that the multipoint source is significantly more efficient under the operating conditions described than is the thin wire. As stated above, the conditions were biased to give the wire field ionizer the highest relative efficiency possible. It is possible that operating the thin wire at higher voltages with larger spacings could improve efficiency, but any possible gains in source efficiency would be offset by losses caused by deceleration and subsequent defocusing of the energetic ions produced. It has been our observation that ionization at lower voltages is desirable for three reasons besides the obvious one of being able to accelerate them into the mass spectrometer. First, experiments measuring the divergence of the ion beam as a function of source potentials show that the emitted beam becomes more divergent at higher voltages. Second, our work in interfacing field ionization sources and quadrupole spectrometers has shown that the problem of high energy neutrals increases sharply with higher source potentials. Third, the frequency and severity of breakdown problems increase as one moves toward high voltages.

It should be noted that the thin wire source can be operated at low voltages with close spacings, although the literature contains no references to other attempts to operate them in this manner. Possibly, with refinement of their mechanical construction to facilitate assembly at close spacings and with sample feed improvements, the thin wire's efficiency might be improved. At present it is doubtful that the thin wire could match the multipoint source's efficiency as field ionizer under the conditions that are optimal for our mass spectrometers. However, the relative insensitivity of the wire sources to abuse makes them attractive when ionization sensitivity is not critical.

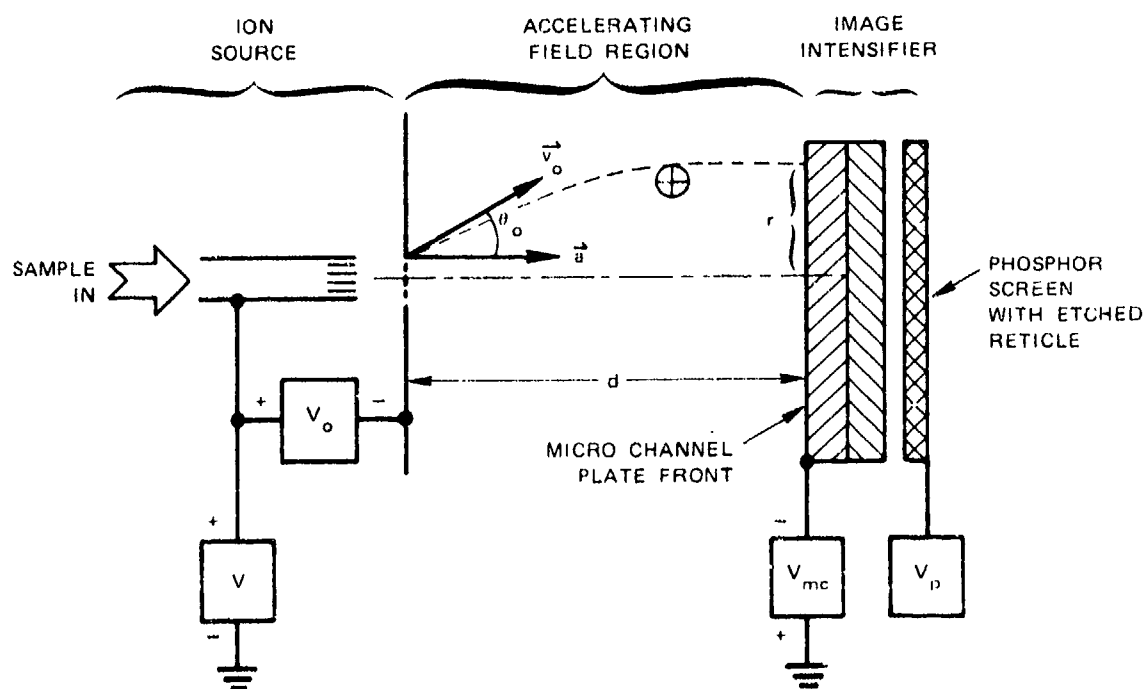
B. Technique for Measuring the Natural Angular Divergence
of Ions Exiting Low Intensity Ionization Sources

For ion optical calculations in mass spectrometers and other ion beam instruments, one frequently employs the so-called Helmholtz-Lagrange law or one of its corollaries applied between two points, a and b, along the path,

$$E_a \, d\Omega_a \, dA_a = E_b \, d\Omega_b \, dA_b \quad (1)$$

where E is the beam energy, $d\Omega$ is the solid angle subtended by the beam, dA is the beam area, and it is assumed that current is conserved and no energy-dispersing devices intervene. In the case of ions exiting an ionization source, the energy and the beam area are generally known at the source exit aperture; however, the angular divergence must be determined experimentally. This presents some difficulties when the ion beam is of low intensity, as in the case of FI sources.

To determine the "natural" angular divergence of the envelope containing the ions produced by the SRI multipoint FI source, we constructed the device shown in figure 33. The FI source is shown schematically at the left. On the right is a microchannel plate-phosphorescent screen combination used as an image intensifier to produce a visible image of the ion beam on the phosphor screen. Between the front microchannel plate and the ionizer exit is a uniform electric field, whose magnitude can be varied either by changing the voltages of the power supplies V , V_o , and V_{mc} , or changing the distance, d , separating the ionizer and the image intensifier. A reticle scribed on the phosphor screen allows the size of the beam striking the image intensifier to be conveniently measured by observing the visible image through the glass wall of the bell jar vacuum system in which the apparatus is mounted.



TA-340622-22b

Figure 33. Schematic of the Apparatus Used to Determine the Angular Divergence of Ions Exiting an Ion Source

Table 4 summarizes the data obtained for three different substrates and various ionizing potentials V_0 . These results are in close agreement with results obtained by other investigators using other techniques.² The variation of beam divergence with ionizing potential is discussed elsewhere.²

The technique presented here is appropriate for beams with an intensity below $\sim 10^{-5}$ A/cm², or where the ion velocity is below $\sim 5 \times 10^7$ cm/sec. However, the technique could readily be applied above these values by direct use of a phosphorescent screen.

C. Improvement of the Interfacing of Quadrupole Mass Filters with Multipoint Field Ionization Sources

Efforts to interface the source with a quadrupole mass spectrometer show that the sensitivity of this instrumental arrangement is limited by a great deal of spectral noise and the loss of intensity that occurs when a highly divergent beam produced at a few keV decelerates to a few eV. It is hypothesized that noise results from the following mechanism. Excited molecules result from neutralization of a certain fraction of the FI produced ions as they pass or collide with the grid, which we can consider as an electron donor past which the ions move. For 3 kV potential grid-to-points the ions pass with a velocity comparable to the orbital velocity of a hydrogenic electron at ~ 100 Å. An electron captured at that velocity and radius forms a Rydberg state with an effective principle quantum number $n^* \approx 11$ and a binding energy $E_n \approx 0.12$ eV obtained from

$$E_n = R_y / (n^*)^2 \quad (7)$$

where R_y is the Rydberg constant.

The free radiative lifetime τ_R of such a state is given by

$$\tau_R \approx \tau_{R_0} (n^*)^3 \quad (8)$$

Table 4. Envelope Divergence Half Angle for Ions Emitted
from Multipoint FI Sources

	1.5 kV	2.0 kV	2.5 kV	3.0 kV
Toluene	24.0° ±0.7°	25.8° ±0.9°	27.7° ±1.1°	28.4° ±1.1°
Thymine		24.2° ±0.9°	25.2° ±0.7°	
Hydrogen		23.4° ±1.0°	23.8° ±0.9°	26.4° ±0.9°

The trajectory of ions exiting the source with some velocity \vec{v}_0 is described by

$$\text{by} \quad d = v_{0\parallel} t + 1/2 a t^2 \quad (2)$$

$$(r - r_0) = v_{0\perp} t \quad (3)$$

$$\text{and} \quad v_{0\perp}^2 + v_{0\parallel}^2 = v_0^2 \quad (4)$$

where d is the separation between the ionizer and the image intensifier, r is the radial coordinate of the point at which the ions strike the image intensifier, r_0 is the radius of the source aperture, a is the axial acceleration of the ions due to the field between the source and the image intensifier, t is the transit time, and $v_{0\perp}$ and $v_{0\parallel}$ are the radial and axial components of \vec{v}_0 , respectively. For $a = 0$, one obtains the exit angle θ_0 from

$$\theta_0 = \text{arc cot } d/(r - r_0) \quad (5)$$

For FI sources, the divergence is so large that it is usually more practical to use an accelerating field to keep the ion beam within the confines of the microchannel plate, in which case the exit angle is obtained from

$$\theta_0 = \text{arc cot } \frac{2dv_0}{(r - r_0)\Delta V} \left\{ \sqrt{1 + \frac{\Delta V}{dv_0} \left(d - \frac{(r - r_0)}{4d v_0} \right)} - 1 \right\} \quad (6)$$

where ΔV is the potential difference across d . In the limit $\Delta V \rightarrow 0$, equation (6) becomes the same as equation (5).

which for $n^* = 11$, yields a lifetime of $\sim 1.4 \mu\text{sec}$, sufficiently long for the excited molecule to enter the quadrupole. The lifetime against FI, τ_I is given by:

$$\tau_I \approx \tau_{I_0} \exp \left(\frac{0.69 I^{3/2}}{F} \right) \quad (9)$$

where I can be replaced by E_n , and F is the effective field at the molecule. Inserting the magnitudes of fields along the beam path and estimating the lifetime for FI from the experiment, one concludes that we observe Rydberg molecules formed with $n^* \geq 30$, corresponding to an ionization potential of $< 0.010 \text{ eV}$ and a free radiative lifetime of $> 30 \mu\text{sec}$.

Ions produced from such fast excited neutrals along the beam path can be only partially decelerated at best and therefore pass through the quadrupole with little or no resolution to produce the spectral noise. At first those neutrals were eliminated by offsetting the FI source from the axis of the quadrupole.⁹ However, since formation of these states is velocity-dependent whereas FI is field dependent, reduction of both-points to counterelectrode voltage and spacing, reduces this noise while maintaining the signal. This eliminates the need for deflection of the beam.

The problem of loss of intensity due to beam divergence was assessed as described in Section V B. The salient information is that the beam divergence is large and that it increases with the point to counterelectrode potential. Consequently, maximum sensitivity for a given FI instrument will be produced by the maximum allowable ion energy and the minimum allowable ionization field. Quadrupoles require ions at a few eV, so the instrumental options are limited in this case. Figure 34 shows two approaches toward utilizing as much of the beam as possible. In Figure 34(b) the ionizer is placed as close as possible to the quadrupole entrance to minimize losses due to loss of brightness

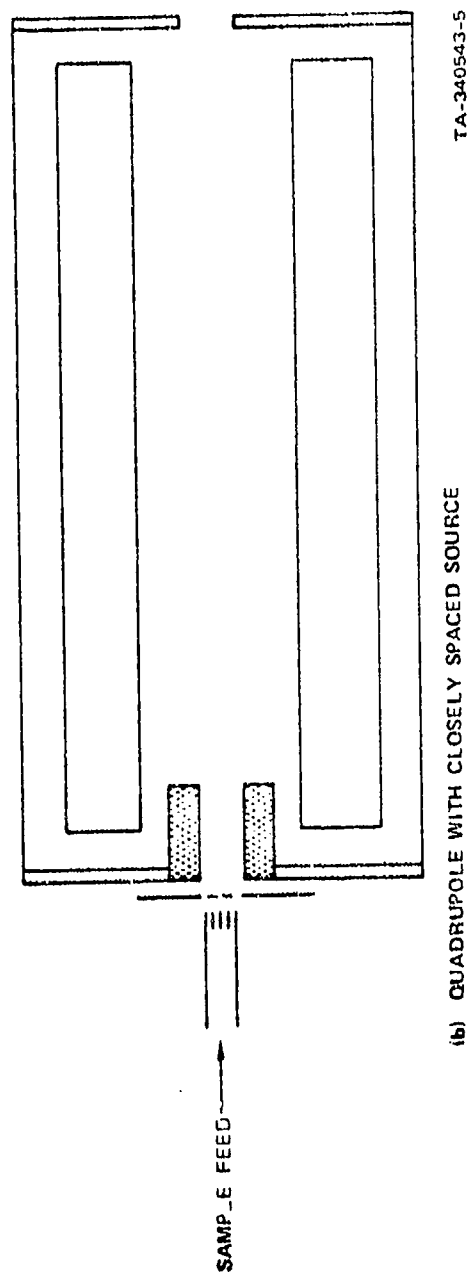
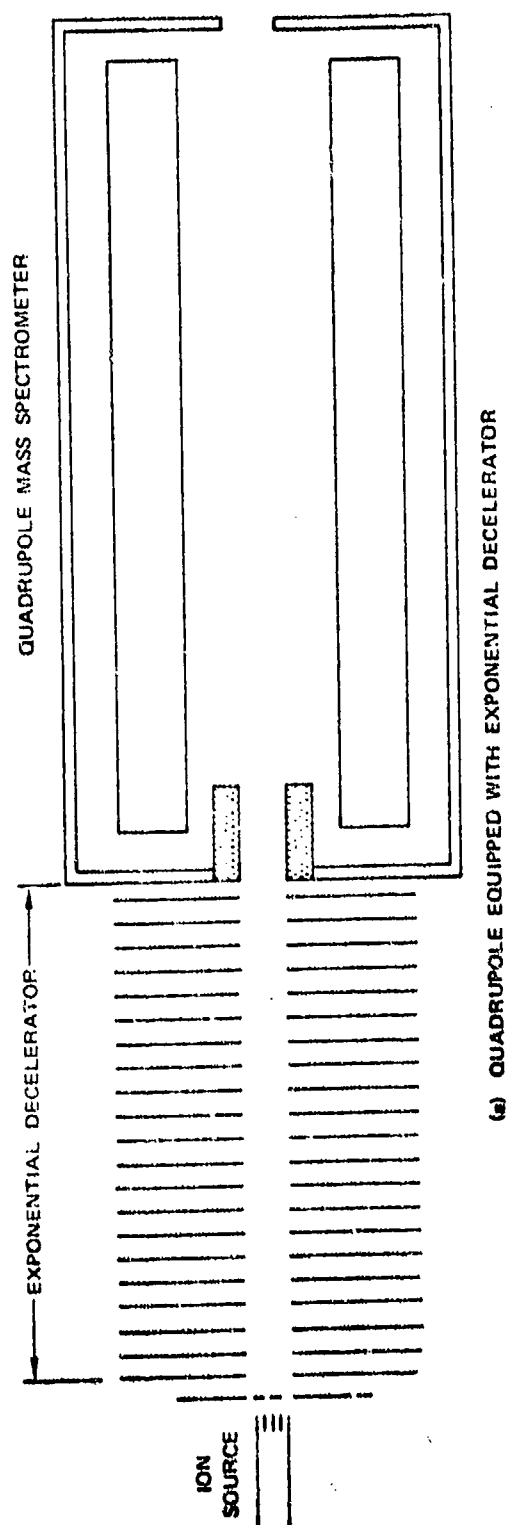


Figure 34. Two Interfacings of Field Ionization Source with Quadrupole Analyzer

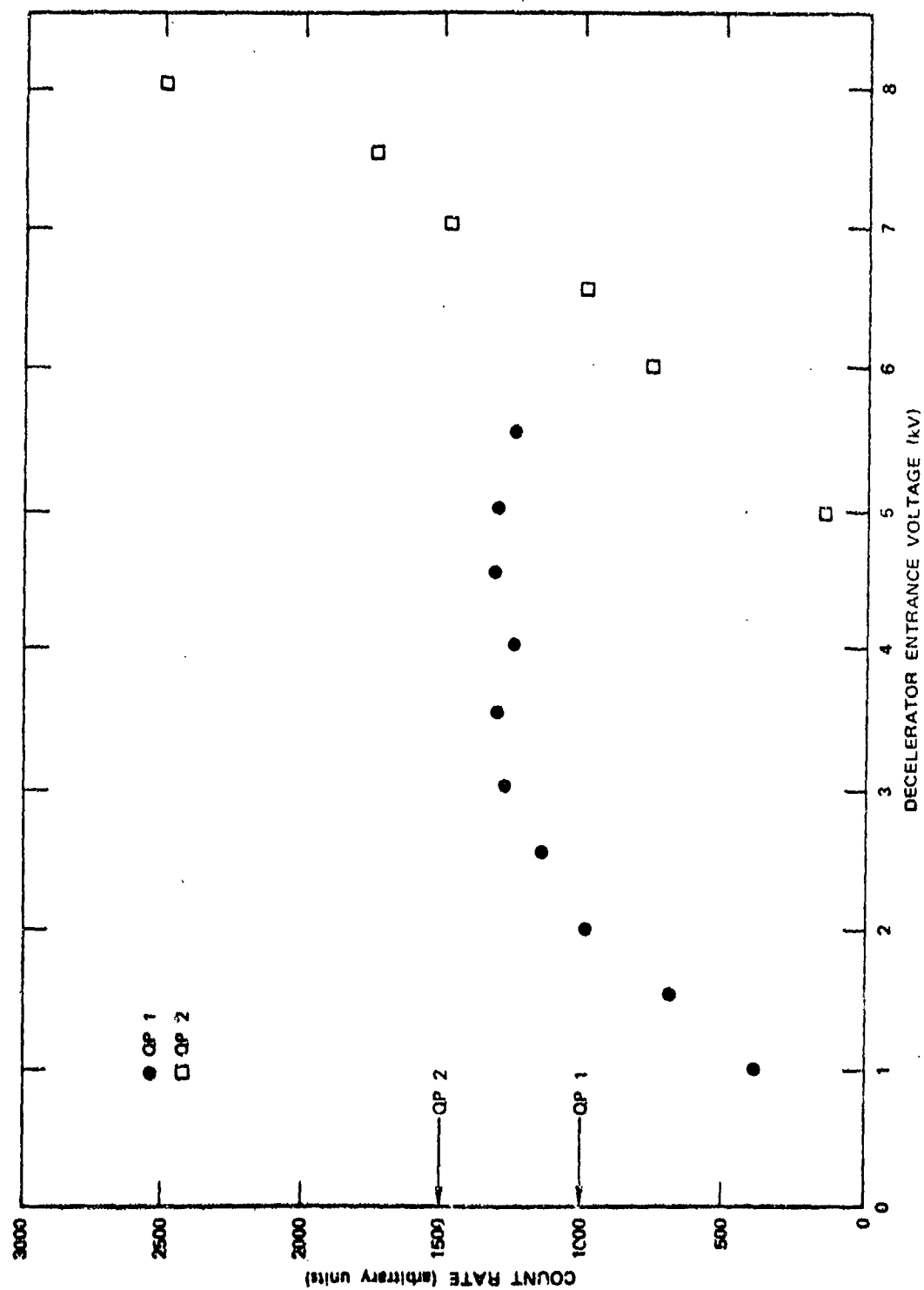
of the divergent beam, which falls off approximately as $1/r^2$. Figure 34(a) illustrates the use of a single stop acceleration-exponential deceleration arrangement. Here an initial acceleration reduces the beam divergence and then, since the quadrupole has a relatively large virtual acceptance aperture, one images a somewhat magnified beam with decreased divergence into the quadrupole.

A comparison of the results of two techniques is shown in Figure 35. The points marked QP 1 and QP 2 indicate count rates obtained from two different quadrupoles with closely spaced sources, and the plotted data show the results from the same quadrupoles with an accel-decel lens. The two quadrupoles behaved dissimilarly; our expectations based on non-mass analyzed experiments lie between these two results. The sensitivity obtained for thymine with either alternative is ~ 55 pg with an overall instrumental efficiency of $\sim 6 \times 10^{14}$ ions/mole.

D. Razor Blade Sources

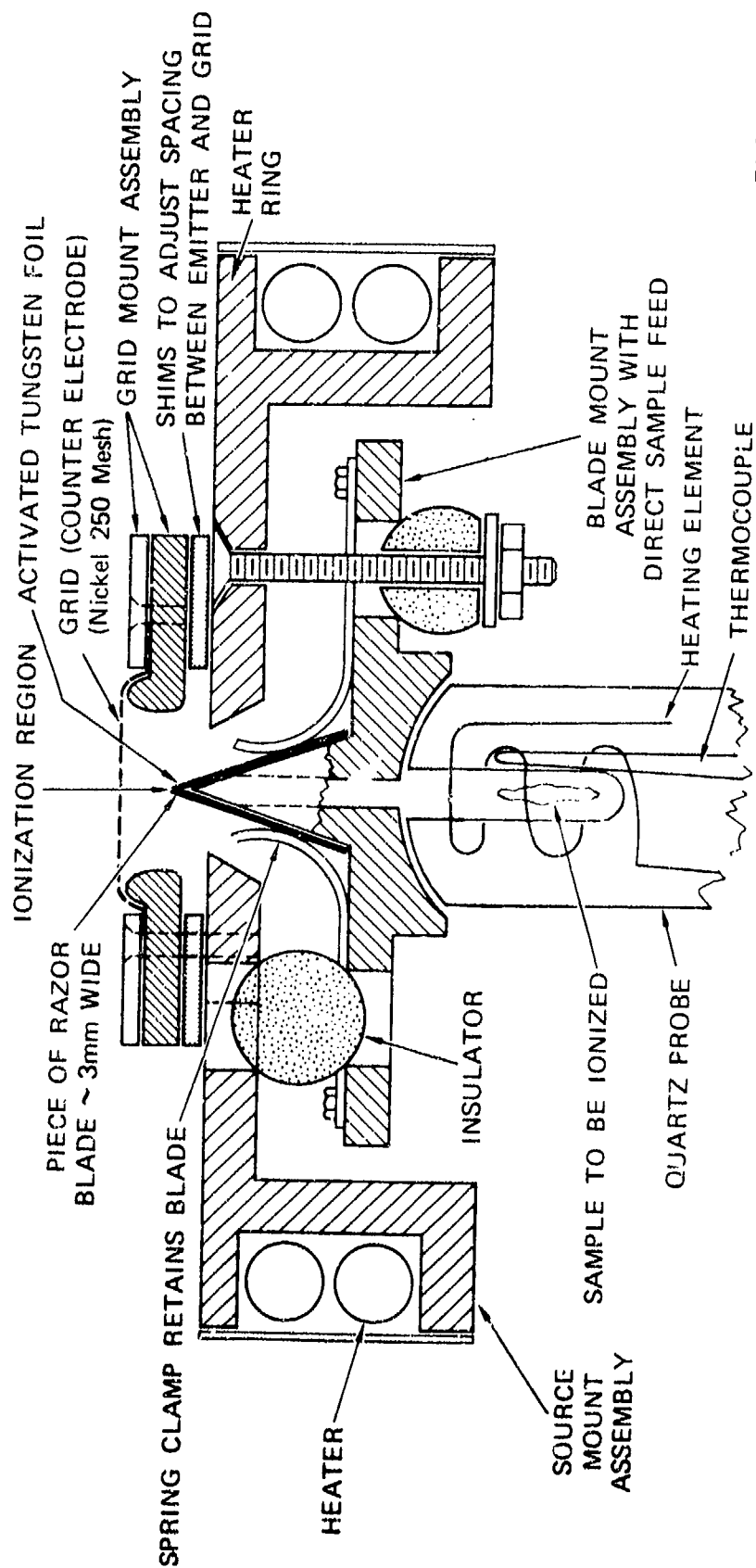
Ionization from a rugged source made from an inert material generating ions in a line aligned with the entrance slit to the sector magnet spectrometer should be an improvement for a portable instrument for general atmospheric sampling. Two sources were assembled from paired razor blade segments mounted close to a screen counterelectrode (Figure 36). The units were tested in a bell jar vacuum to confirm ionization and to initiate activation of the ionizing sites.

Initial resolution was high (~ 400) with the entrance slit at 2 mm. Closing the slit decreased the ion intensity at the detector without significantly increasing resolution. With the slit closed to 0.2 mm, the intensity had fallen to 1/10 the full slit intensity, and resolution had risen to 500. Sensitivity of the source to standard laboratory chemicals used to test sources (xylene and thymine) indicate that the sources were about 1/4 as sensitive as a well-conditioned multipoint source, even though the blades were not themselves



TA-340543-4

Figure 35. Mass Analyzed Count Rate versus Decelerator Entrance Voltage



TA-340522-236R1

Figure 36. Razor Blade Slit Type Field Ionization Source

fully conditioned. This result indicates that the blade source may prove to be as sensitive as the multipoint source. Long-term conditioning on another instrument indicated a somewhat higher sensitivity to thymine for the razor blade.

VI CONCLUSIONS AND RECOMMENDATIONS

The experimental results presented in this report indicate that GB or VX could be detected in air at the ppt level by mass spectrometry if the following two constraints were overcome:

- (1) The problem of chemical background, which limits the level of detectability, even with the most specific ionization techniques, to 1 ppb.
- (2) The problem of adsorption on surfaces of the phosphonates at the sub-ppb levels, which limits the response time of any detection system.

If the chemical contaminants are removed, it will not be necessary to improve the sensitivity of the existing detection systems; still, an improvement by up to two orders of magnitude is feasible, if called for. At present, we estimate that our overall ionization-times-detection efficiency is higher than 6×10^{15} ions/mole (10^{-8} ions/molecule). This could be increased to up to 10^{18} ions/mole by better interfacing of the ionization source with the mass analyzer. However, as we shall see below, any effective chemical purification process involves a concentration stage, which in turn increases the detection sensitivity without any modifications of the mass spectrometric instrumentation.

We are now in a position to conceptualize a detection system that should overcome the limitations described above. The system consists of a temperature programmable short adsorption column (packed with appropriate adsorbant) connected through a three-way valve to a jet separator, which leads directly into the ionization source. The organic phosphorous compound in air is then adsorbed from the air on the column at room temperature. The column is then flushed with helium while the temperature is increased to a predetermined value. This procedure will desorb most organic materials, which are less polar and more volatile than GB.

After this stage is reached, the valve that connects the column with the jet separator is opened and the temperature is rapidly increased to desorb the phosphonates, which are then introduced with the He carrier into the ionization source. Instead of helium, we may also use H_2 as the carrier gas. This gives us the additional option of using a palladium tube separator and gaining transfer efficiency of the GB from the desorption column into the ionization source.

Let us consider a quantitative example. Four liters of air containing a concentration of 1 ppt GB are passed over the column in 2 minutes. The column is then heated while being flushed with He (100 ml/min) for 2 minutes. The column is then heated to a higher temperature for 2 minutes to release the GB into the mass spectrometer. In total, we originally had 1.5×10^{-13} mole or 10^{11} molecules of GB. Assuming an adsorption efficiency of 90%, a loss of 10% of GB during the flushing stage, and a 50% loss in the separation stage, we would have 4×10^{10} molecules of GB introduced into the ionization source within 1 minute. Assuming an additional pyrolytic loss of 50%, which may be necessary to cut down the residence time in the inlet system, and an overall detection efficiency of 10^{-8} (which we achieve routinely at present), we would obtain 200 counts at 140 amu over a period of less than 2 minutes, with a total background of less than 20 counts.

To standardize the ionization efficiency, we will continuously bleed in a low concentration of diethyl benzene (134 amu) and beam-switch between masses 134 and 140 with a duty cycle of 1:20. A loss of 5% in sensitivity is worthwhile to ascertain the efficiency of the mass spectrometric system.

An inlet system could be constructed with three adsorption-desorption columns operating in sequence so that the mass spectrometer would measure samples in an uninterrupted manner, monitoring another sample every two

minutes. Although such a system would not be a "real time" monitor, it would provide continuous information on the concentration of GB in air (every 2 minutes) with an average time lag of 5 minutes.

Evidently we may also use the batch desorption concentrator technique in conjunction with a negative ion source, whether "inverse" field ionization or electron impact. As things stand today, we believe that electron impact will induce excessive fragmentation and therefore higher chemical background, even following a preliminary desorption clean-up, because many higher molecular weight materials will adsorb and desorb together with the GB. These will not interfere with field ionization, where virtually only molecular ions are formed; nor will they interfere with negative ion formation by electron capture in a field, where only materials with high electron affinity will produce ions. Electron impact, however, produces many free radicals, and many of these have significant electron affinity and will form negative ions.

Negative ion chemical ionization will be another possible ionization technique, once the preseparation technique has been worked out. In this case, we would use $3F_6^-$ as the primary electron donor.

The proposed system differs significantly from a GC-MS arrangement. First, it takes much less time to concentrate the agent from a larger air sample and far less time for clean-up. Second, it allows the handling of much smaller amounts of material. By glc, it is impractical to fractionate quantities of material smaller than 10^{-10} g, whereas the proposed total adsorption-desorption system can go down to subpicogram quantities. Third, a GC-MS system requires a minicomputer to obtain meaningful information, because if the total sample is less than a nanogram, it cannot be split, and there is no detector other than a mass spectrometer that can detect its arrival. Using a glc necessitates repeated scanning

and computation analysis of the arrival time of the desired material, using the arrival time of other constituents as markers. Therefore, even if the concentration of GB or VX were high enough to allow glc separation, and even if the time factor were not critical, we should have to increase the investment in instrumentation by some \$25,000 to \$30,000 compared with our proposed system.

An integrating batch system has a number of advantages over continuous monitoring. First, it has a higher sensitivity and lower background by two to three orders of magnitude, even with the existing instrumentation. Second, it promises much longer durability of the field ionizer because we introduce in this case mainly helium as carrier gas and practically no oxygen. Third, in view of our past experience with the response time of silicon-rubber inlet systems, it is unlikely that the response time attainable on a continuous monitoring "real time" system would be shorter than 5 minutes. (We cannot use a jet separator on a continuous monitoring system because of the relatively higher molecular weight of O_2 and N_2 .) Fourth, if for any reason it is desirable to increase the sensitivity range of the detection system at any given time, the rate of air flow can be doubled (with minimal sacrifice of adsorption efficiency) and the time of collection increased from 2 minutes to 10 minutes.

If the ionization efficiency of field ionization sources is increased, which we hope to achieve in the foreseeable future, and if the interfacing between these ionizers and the mass analyzer is improved, which we hope to happen as a result of a collaborative effort with Perkin-Elmer, the sensitivity of detection of GB or VX in air could increase at least to one part in 10^{14} .

LITERATURE CITED

1. J. N. Domico, R. P. Barron, and J. A. Sphon, *Int. J. Mass Spec. Ion Phys.* 2, 161 (1969).
2. H. D. Beckey, Field Ionization Mass Spectrometry (Pergamon Press, London, 1971).
3. E. W. Muller, *Phys. Rev.* 102, 618 (1965).
4. M. Anbar and W. H. Aberth, *Anal. Chem.* 46, 59A (1974).
5. Gilbert A. St. John and Michael Anbar, "Determination of Subpicogram Amounts of Chemical Agents in the Atmosphere," Edgewood Arsenal Contract Report No. EC-CR-74028, SRI Project 3122 (August 1974).
6. C. A. Spindt, *J. Appl. Phys.* 39, 3504 (1968); W. H. Aberth, C. A. Spindt, and R. R. Sperry, *Proceedings of the 21st Annual Conference on Mass Spectrometry and Allied Topics*, San Francisco (May 1973) p. 453.
7. G. A. St. John and M. Anbar, *Proceedings of the 21st Annual Conference on Mass Spectrometry and Allied Topics*, San Francisco (May 1973) p. 139.
8. M. Anbar and G. A. St. John, "Formation of Negative Ions Under Inverted Field Ionization Conditions," *Science* 97, 24 (1975).
9. H. L. Brown and M. Anbar, "The Formation of Superexcited Organic Species in Field Ionization Sources," *Int J. Rad. Phys. Chem.* 7, 281 (1975).

DISTRIBUTION LIST

Commander
Edgewood Arsenal
Attn: SAREA-CL-DD/Dr. C. S. Harden 33 copies

Commander, Edgewood Arsenal
Attn: SAREA-TL-L 3 copies
Attn: SAREA-TS-R 1 copy
Aberdeen Proving Ground, MD 21010

Commander, US Army Armament Command
Attn: DRSAR-RDT 1 copy
Rock Island, ILL 61201

Defense Documentation Center
Cameron Station
Alexandria, VA 22314 12 copies